

## High-Energy Proton Scattering and the Structure of Light Nuclei\*

ROBERT H. BASSEL AND COLIN WILKIN†

Brookhaven National Laboratory, Upton, New York 11973

(Received 23 April 1968)

The elastic and total cross sections of 1-BeV protons on  $H^2$ ,  $He^4$ ,  $C^{12}$ , and  $O^{16}$  are analyzed, in conjunction with the corresponding electron scattering measurements, on the basis of Glauber's high-energy approximation. This leads to information which cannot be obtained from the electron data alone.

### I. INTRODUCTION

OVER the past fifteen years, high-energy electron scattering experiments have provided much valuable information on the structure of nuclei.<sup>1</sup> For a light nucleus, this electromagnetic interaction seems to be reasonably well described by the first Born approximation, apart from quite small corrections arising in the vicinity of minima in the angular distributions. For elastic scattering, however, the Born approximation depends only upon the charge distribution in the nucleus, that is, upon a single-particle density function. It is seen, therefore, that the results of elastic electron scattering can shed no light on the possibility of nucleon-nucleon correlations in the nucleus. The effects of such correlations can be important if we consider the transitions to excited levels in the nucleus. For example, using the closure approximation on the final nuclear states and summing over both the elastic and quasielastic cross sections, it is possible to get an expression which depends upon a two-particle rather than a one-particle density function. However, the evaluation of this sum rule is difficult experimentally. Corrections have to be made for bremsstrahlung and pion production, and even then the result is found not to be too sensitive to the correlation function. To investigate clearly this correlation, we really need a probe which has an appreciable probability of interacting at least twice as it passes through the nucleus. Simple geometric arguments of the solar-eclipse genre suggest that for a 1-BeV proton the amplitude for a second interaction might be of the order of 20% of the single-interaction term in the forward direction even for a nucleus as light as  $He^4$ . This figure rises to around 50% for  $O^{16}$ . More important still, it will be shown in Sec. II that for elastic scattering the double-interaction amplitude falls off more slowly with angle away from the forward direction than does the single. It is more economical to compound a large-angle proton-nucleus scattering from two smaller deflections rather than just one large-angle proton-proton scattering. There are thus regions of the angular distribution where the double scattering predominates. In the interference region where the single and double scattering

are comparable, the shape of the cross section depends critically on the relative phase. Since at these energies the proton-nucleon amplitudes are dominantly imaginary, it can be shown that this interference is primarily destructive. This leads to a typical diffraction pattern, the first minimum being due, in the main, to the interference between single and double scattering, the second to double and triple, etc. The sensitivity of the positions of the minima, and the heights of the subsidiary maxima, on the nucleon wave function is of great practical importance in the analysis of the experimental data.

In the hope of discovering more about the structure of nuclei in general and correlations in particular, the Brookhaven group performed a series of experiments with a beam of 1-BeV protons.<sup>2</sup> A great many data were accumulated on the elastic differential and total cross sections in  $H$ ,  $D$ ,  $He^4$ ,  $C^{12}$ ,  $O^{16}$ , as well as on the excitation of various nuclear levels, nuclear breakup,  $(p,d)$  and  $(p,2p)$  reactions, etc. To separate, say, the 4.4-MeV state of  $C^{12}$  from the ground state, very good resolution is required. This was provided in these experiments by the high angular resolution of wire spark chambers in conjunction with the extreme energy stability of the external beam of the Cosmotron.

It is the purpose of the present paper to make a detailed analysis of the elastic-scattering and total cross-section results under the assumption that the nuclei in question are spherical. We defer to a later paper problems associated with nuclear deformation which are particularly important in the case of carbon. A preliminary attempt is also made to understand the excitation of the first  $2^+$  state in carbon.

The dynamical basis of our calculation is the multiple-scattering model proposed many years ago by Glauber.<sup>3-6</sup> This is described in detail in Sec. II and is

<sup>2</sup> H. Palevsky, in *High Energy Physics and Nuclear Structure*, edited by G. Alexander (North-Holland Publishing Co., Amsterdam, 1967), p. 151; H. Palevsky *et al.*, Phys. Rev. Letters **18**, 1200, (1967); G. W. Bennett *et al.*, *ibid.* **19**, 387 (1967); G. J. Igo *et al.*, Nucl. Phys. **B3**, 181 (1967); H. Palevsky and J. L. Frieses (private communication).

<sup>3</sup> R. J. Glauber, in *Lectures in Theoretical Physics*, edited by W. E. Brittin and L. G. Dunham (Interscience Publishers, Inc., New York, 1959), Vol. 1, p. 315; Phys. Rev. **100**, 242 (1955).

<sup>4</sup> V. Franco and R. J. Glauber, Phys. Rev. **142**, 1195 (1966); V. Franco and E. Coleman, Phys. Rev. Letters **17**, 827 (1966).

<sup>5</sup> H. Feshbach, *International School of Physics "Enrico Fermi"* (Academic Press Inc., New York, 1967), Course No. 38.

<sup>6</sup> C. Wilkin, in *Summer Institute in Nuclear and Particle Physics* (W. A. Benjamin, Inc., New York, 1968).

\* Work performed under the auspices of the U. S. Atomic Energy Commission.

† Present address: Department of Physics, University College, London, England.

<sup>1</sup> See, for example, R. Hofstadter, *Nuclear and Nucleon Structure* (W. A. Benjamin, Inc., New York, 1963).

there applied to a simplified model of the nucleus. An exposition of the theory in terms of diagrams can be found in Sec. III, where the nature of the approximations is presented in greater depth. Section IV deals with the modifications to the simplified model which are necessary to explain the helium results. Included there also is an analysis of the proton-proton cross section and ways to parametrize it. Oxygen is discussed in Sec. V in terms of both a simple product ground-state wave function and an antisymmetrized wave function. A similar approach is then tried for carbon. Although at first sight the case of deuterium would appear to be the most simple, there are in fact complications and it will be dealt with last, in Sec. VII. Section VIII is devoted to a summary of our results and to some thoughts about future experiments and calculations.

## II. GLAUBER THEORY OF HIGH-ENERGY SCATTERING

The most prominent feature of high-energy scattering of strongly interacting particles is the very strong forward diffraction peak. The description of this phenomenon on the basis of a partial-wave expansion would require very many terms with a conspiracy of delicate cancellations. On the other hand, this feature occurs quite naturally in the same semiclassical picture of scattering.<sup>3-6</sup> We there think of a particle trajectory passing through an absorbing sphere and giving rise to a diffraction pattern, in complete analogy with classical optics. The trajectory in this type of model is specified completely by the classical impact parameter  $b$ . Consequently, if we assume that the elastic proton-proton amplitude is spin-independent, then we can write down a representation for it in terms of the impact parameter:

$$f(\mathbf{q}) = \frac{ik}{(2\pi)} \int d^{(2)}b e^{i\mathbf{q}\cdot\mathbf{b}} (1 - e^{2i\chi(\mathbf{b})}), \quad (2.1)$$

where the integration is over a plane perpendicular to the beam direction. But because of the assumption of spin independence the phase shift  $\chi(\mathbf{b})$  depends only upon the magnitude of  $\mathbf{b}$ , so that the representation (2.1) simplifies to

$$f(q) = ik \int_0^\infty b db J_0(qb) (1 - e^{2i\chi(b)}). \quad (2.2)$$

This description can be obtained by writing down the partial-wave expansion in the c.m. frame and identifying the impact parameter in terms of the angular momentum by

$$b = (l + \frac{1}{2})/k. \quad (2.3)$$

Equation (2.2) then follows if one goes to the limit of high energies and small scattering angles. Although in this way we can justify the representation for the c.m. system, for small scattering angles the relativistic trans-

formations are extremely simple,<sup>4</sup> and so (2.1) or (2.2) should also be valid in the laboratory system, provided that we interpret  $k$  as the laboratory momentum and

$$(d\sigma/d\Omega)_{\text{lab}} = |f(q)|^2. \quad (2.4)$$

We must, however, keep the c.m. relation

$$q^2 = -t. \quad (2.5)$$

Thus in all our formulas  $q^2$  must finally be interpreted as the four-momentum transfer and not the three-momentum. With our normalization, the optical theorem becomes

$$\sigma_T = (4\pi/k) \text{Im}[f(0)]. \quad (2.6)$$

Provided that the scattering is only through small angles, the impact-parameter transform, Eq. (2.1), has the approximate inversion

$$\Gamma(\mathbf{b}) \equiv (1 - e^{2i\chi(\mathbf{b})}) = \frac{1}{(2\pi ik)} \int e^{-i\mathbf{q}\cdot\mathbf{b}} f(\mathbf{q}) d^{(2)}q, \quad (2.7)$$

where the integration is over a plane perpendicular to  $\mathbf{k}$ . A more precise inversion would involve the integration over the surface of a sphere which more accurately represents the locus of the momentum transfer  $\mathbf{q}$  for fixed energy and varying angle. The correction due to this will be quite small, provided that  $f(\mathbf{q})$  is sharply peaked forward and we do not look at too large angles.

All that remains to do now is calculate the phase shifts  $\chi(b)$ . In optical calculations one assumes that the total phase shift as a photon passes through a lens, for example, is just the sum of the infinitesimal phase shifts  $\delta\chi$  taken along the trajectory  $\mathbf{r}$ . In fact,

$$\delta\chi = n(\mathbf{r}) \mathbf{k}(\mathbf{r}) \cdot \delta\mathbf{r}, \quad (2.8)$$

where  $n(\mathbf{r})$  is the local refractive index and  $\mathbf{k}(\mathbf{r})$  is the local wave vector. The crucial part of Glauber's theory is to assume that a good approximation to the phase shift can be obtained, not by adding up the elemental phase shifts along the true trajectory, but rather along a straight line, along the undeviated beam direction. This implies that the phase shift due to a lens is independent of whether or not there is other refracting material around or not. As a consequence, the phase change at impact parameter  $b$  due to a two-lens system is just the sum of the phase shifts of each lens taken separately, of course at the appropriate values of the impact parameters.

Let us now consider the scattering of protons from an ensemble of nucleons inside a nucleus. Suppose that during the passage of the fast particle the motion of the positions  $\mathbf{r}_j$  may be neglected. The arguments of the preceding paragraph lead one to postulate that the nuclear phase shift for a particular configuration  $\mathbf{r}_1, \dots, \mathbf{r}_A$  of the nucleons is just the sum of the individual

phase shifts

$$\chi_N(\mathbf{b}, \mathbf{r}_1, \dots, \mathbf{r}_A) = \sum_{j=1}^A \chi_j(\mathbf{b} - \mathbf{s}_j), \quad (2.9)$$

where  $\epsilon_j$  is the component of  $\mathbf{r}_j$  perpendicular to the beam (see Fig. 1).

For convenience define the operators

$$\Gamma_j(b) = (1 - e^{2i\chi_j(b)}) \quad (2.10)$$

for the nucleons and

$$\Gamma_N(\mathbf{b}, \mathbf{r}_1, \dots, \mathbf{r}_A) = (1 - e^{2i\chi_N(\mathbf{b}, \mathbf{r}_1, \dots, \mathbf{r}_A)}) \quad (2.11)$$

for the nucleus. Now since we do not observe the positions of the nucleons in the nucleus we must average the scattering operator  $\Gamma_N$  over the positions of the  $A$  nucleons. However, this operator can generate not only elastic scattering, but also transitions to other states of the  $A$ -nucleon system, such as  $A(p, 2p)A-1$ . Hence if  $|i\rangle$  is the initial ground state and  $|f\rangle$  is the final ground or excited state of the nucleus, then the transition amplitude becomes

$$F_{fi}(\mathbf{q}) = \frac{ik}{(2\pi)} \int e^{i\mathbf{q} \cdot \mathbf{b}} d^{(2)}\mathbf{b} \langle f | \Gamma_N(\mathbf{b}, \mathbf{r}_1, \dots, \mathbf{r}_A) | i \rangle. \quad (2.12)$$

We now have a sufficient dynamical basis to perform a calculation of proton-nucleus scattering, given the proton-nucleon amplitudes. The latter are fed into the right-hand side of (2.7) to give the proton-nucleon impact-parameter amplitudes, which, using (2.10) and (2.11), lead to the proton-nucleus impact-parameter amplitude. The circuit is closed by Eq. (2.12), which gives the proton-nucleus scattering amplitude. This procedure can be summarized in one equation:

$$\begin{aligned} F_{fi}(\mathbf{q}) = & \left( \frac{ik}{2\pi} \right) \int e^{i\mathbf{q} \cdot \mathbf{b}} d^{(2)}\mathbf{b} \int d^3\mathbf{r}_1 \dots d^3\mathbf{r}_A \\ & \times \psi_f^*(\mathbf{r}_1, \dots, \mathbf{r}_A) \delta^{(3)}\left(\frac{1}{A}\sum \mathbf{r}_j\right) \\ & \times \left[ 1 - \prod_{j=1}^A \left( 1 - \frac{1}{(2\pi ik)} \int e^{-i\mathbf{q}' \cdot (\mathbf{b} - \mathbf{s}_j)} f_j(\mathbf{q}') d^{(2)}\mathbf{q}' \right) \right] \\ & \times \psi_i(\mathbf{r}_1, \dots, \mathbf{r}_A), \quad (2.13) \end{aligned}$$

where  $\psi_{i(f)}$  is the wave function of the initial (final) nuclear state. The over-all delta function in the nuclear c.m. variable  $\sum \mathbf{r}_j$  ensures that the final nucleus is in a state of well-defined momentum.<sup>7</sup> Because of this condition the wave functions  $\psi$  have to be calculated with respect to the c.m. of the nucleus. Most of the rest of this paper will be devoted to the application of this

<sup>7</sup> R. J. Glauber, in *High Energy Physics and Nuclear Structure*, edited by G. Alexander (North-Holland Publishing Co., Amsterdam, 1967), p. 311.

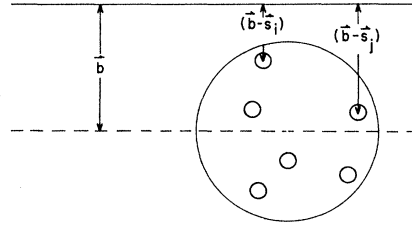


FIG. 1. Proton-nucleus scattering at impact parameter  $\mathbf{b}$  is compounded out of many proton-nucleon scattering at impact parameters  $\mathbf{b} - \mathbf{s}_i$ .

equation to the various nuclei studied by the Brookhaven group.<sup>2</sup>

It cannot be emphasized too strongly that in deriving Eq. (2.13) we explicitly neglected the spin dependence of the nucleon-nucleon amplitude, and treated the isospin in a nonrigorous way.

If the product over the nucleus  $j$  in Eq. (2.13) is expanded, then we see that the nuclear amplitude  $F$  can be represented as a polynomial in the nucleon amplitude  $f$ . This can be interpreted as a multiple-scattering expansion; the lowest order is single scattering, second order is double scattering, etc. But since the order of the polynomial is  $A$ , there can at most be an  $A$ -fold scattering. The physical reason for this is that since the proton-nucleon amplitudes are assumed to be very sharply peaked in the forward direction, it is unlikely that the proton would scatter from nucleon  $A$  to  $B$  and back to  $A$  again.

A particularly simple result holds for the lowest-order terms, the so-called impulse approximation. Here one of the Fourier transforms is the inverse of the other and we are left with

$$\begin{aligned} F_{fi}(\mathbf{q}) = & \sum_{j=1}^A f_j(\mathbf{q}) \int e^{i\mathbf{q} \cdot \mathbf{s}_j} \psi_f^*(\mathbf{r}_1, \dots, \mathbf{r}_A) \psi_i(\mathbf{r}_1, \dots, \mathbf{r}_A) \\ & \times \delta^{(3)}\left(\frac{1}{A}\sum \mathbf{r}_j\right) d^3\mathbf{r}_1, \dots, d^3\mathbf{r}_A. \quad (2.14) \end{aligned}$$

In this approximation the proton-nucleus amplitude is proportional to some proton-nucleon amplitude multiplied by a form factor. For a light nucleus, Eq. (2.14) would describe electron scattering quite well, but for a strongly interacting particle the multiple scatterings involve quite large corrections. Note that it is very likely for the light nuclei we are concerned with that the proton and neutron distributions in the nucleus are very similar, that is, isospin is a good quantum number.

Let us now study a rather oversimplified model of a nucleus. For elastic scattering, we require only the density distribution of the ground state:

$$\rho(\mathbf{r}_1, \dots, \mathbf{r}_A) = \psi_G^*(\mathbf{r}_1, \dots, \mathbf{r}_A) \psi_G(\mathbf{r}_1, \dots, \mathbf{r}_A). \quad (2.15)$$

We now make the drastic assumption that the nucleons in the nucleus are completely uncorrelated, so that the

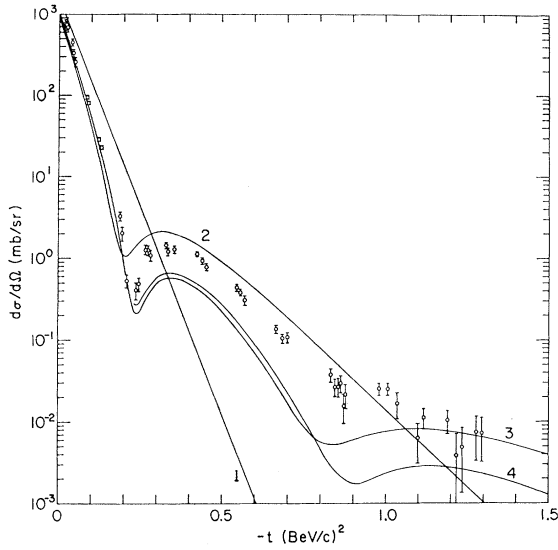


FIG. 2. Differential cross section for elastic proton-He<sup>4</sup> scattering at 1 BeV; the experimental data are from Ref. 2. The theoretical predictions are from Eq. (2.21) with  $\alpha^2=0.535 \text{ F}^{-2}$ ,  $\beta^2=5.45 \text{ (BeV/c)}^{-2}$ ,  $\sigma=44 \text{ mb}$ , and  $\rho=-0.3$ . Curve 1 represents the contribution of single scattering (impulse approximation), curve 2 represents single plus double, etc.

density function factors into the product of  $A$  terms

$$\rho(\mathbf{r}_1, \dots, \mathbf{r}_A) = \rho(\mathbf{r}_1) x \cdots x \rho(\mathbf{r}_A). \quad (2.16)$$

Inserting this into Eq. (2.13) we see that all the  $\mathbf{r}_j$  integrations would factorize if it were not for the c.m. delta function. By use of an ingenious transformation due to Gartenhaus and Schwartz,<sup>8</sup> it is possible to remove this delta function, but the result is only simple if we are dealing with harmonic-oscillator wave functions. We therefore take all the  $A$  nucleons to be  $1s$  bound states in a harmonic well of range  $1/\alpha$ . Then

$$\rho(\mathbf{r}_j) = (\alpha^2/\pi)^{3/2} e^{-\alpha^2 r_j^2}. \quad (2.17)$$

The Gartenhaus-Schwartz prescription is now to neglect the delta-function constraint and multiply the remainder by  $\exp(q^2/4A\alpha^2)$ . This recipe is also valid if the nucleons are in  $1P$  or higher waves and we shall have occasion to use it again elsewhere. With these assumptions the proton-nucleus elastic amplitude (2.13) becomes

$$F(\mathbf{q}) = \frac{ik}{(2\pi)} e^{q^2/4A\alpha^2} \int e^{i\mathbf{q}\cdot\mathbf{b}} d^{(2)}\mathbf{b} \times \left\{ 1 - \prod_{j=1}^A \left[ 1 - \frac{1}{2\pi ik} \int d^{(2)}\mathbf{q}' \times e^{-i\mathbf{q}'\cdot\mathbf{b}} e^{-q'^2/4\alpha^2} f_j(q') \right] \right\}. \quad (2.18)$$

To go much further we must have some parametrization of the nucleon-nucleon amplitudes  $f_j$ . As will be

discussed in detail in Sec. IV, for not too large values of  $|t|$  [say, less than  $0.4 \text{ (BeV/c)}^2$ ], the proton-proton cross section falls exponentially with  $|t|$ . Therefore, we take

$$f_j(q) = (ik\sigma_j/4\pi)(1-i\rho_j)e^{-\beta^2 q^2/2}. \quad (2.19)$$

By taking  $\sigma_j$  as the total proton-proton cross section, Eq. (2.19) satisfies the optical theorem (2.6). Note that the relative real part of the amplitude  $\rho_j$  is taken as being independent of momentum transfer  $q$ . Since the present model is so simplified, let us go even further and forget the difference between protons and neutrons. Thus the parameters  $\sigma$ ,  $\rho$ , and  $\beta$  of Eq. (2.19) are taken to be the average of those for neutrons and protons. This parametrization can be fed into Eq. (2.18) to give

$$F(\mathbf{q}) = \left( \frac{ik}{2\pi} \right) e^{q^2/4A\alpha^2} \int e^{i\mathbf{q}\cdot\mathbf{b}} d^{(2)}\mathbf{b} \times \left[ 1 - \prod_{j=1}^A \left( 1 - \frac{\sigma(1-i\rho)\alpha^2 \exp[-\alpha^2 b^2/(1+2\alpha^2\beta^2)]}{2\pi(1+2\alpha^2\beta^2)} \right) \right]. \quad (2.20)$$

Since there is no explicit  $j$  dependence in the product of Eq. (2.20), this simply becomes a quantity to the power  $A$ . This can be expanded in a power series in  $\sigma$  and the Fourier transforms done analytically.

$$F(q) = \left( \frac{ik}{2\pi} \right) \left( \frac{1+2\alpha^2\beta^2}{\alpha^2} \right) e^{q^2/4A\alpha^2} \sum_{j=1}^A \binom{A}{j} \frac{(-1)^{j+1}}{j} \times \left[ \frac{\sigma(1-i\rho)\alpha^2}{2\pi(1+2\alpha^2\beta^2)} \right]^j \exp \left[ -\frac{(1+2\alpha^2\beta^2)q^2}{4\alpha^2 j} \right]. \quad (2.21)$$

This formula, first derived by Cys $\acute{z}$  and Le $\acute{s}$ niak,<sup>9,10</sup> has all the general properties associated with more complicated models of the nucleus. As was stressed earlier, it is a polynomial in the nucleon-nucleon interaction, the expansion parameter being roughly  $X \approx \sigma\alpha^2/2\pi$ . This is because the relative real part  $\rho$  is comparatively small at these energies and the proton size ( $\sim\beta^2$ ) is much less than the nuclear size ( $\sim\alpha^{-2}$ ). If we put in typical numbers for proton scattering off He<sup>4</sup>, using the value of  $\alpha^2$  deduced from electron scattering, we find  $X \sim 0.25$ . In the forward direction, therefore, the single-scattering terms are the most important, but examination of the exponent in (2.21) shows that single scattering falls off more rapidly with angle than does double scattering, so that some value of  $q^2$  the double- and single-scattering contributions will be equal in magnitude. For larger  $q^2$ , the double will be dominant until, for even larger  $q^2$ , the triple takes over, etc. As was remarked above, at these energies  $\rho$  is quite small (at most 30%). Conse-

<sup>9</sup> W. Cys $\acute{z}$  and L. Le $\acute{s}$ niak, Phys. Letters **24B**, 227 (1967); W. Cys $\acute{z}$ , in *High Energy Physics and Nuclear Structure*, edited by G. Alexander (North-Holland Publishing Co., Amsterdam, 1967).

<sup>10</sup> R. H. Bassel and C. Wilkin, Phys. Rev. Letters **18**, 871 (1967).

<sup>8</sup> S. Gartenhaus and C. L. Schwartz, Phys. Rev. **108**, 482 (1957).

quently, the  $(-1)^{j+1}$  factor makes the odd scatterings be principally out of phase with the even ones. If  $\rho$  were zero, then the amplitude would have zeros, but with  $\rho \sim 0.3$ , the resulting cross section just shows sharp minima. The application of Eq. (2.21) to the case of  $\text{He}^4$ , viz.,  $A=4$ ,  $\alpha^2=0.535 \text{ F}^{-2}$ , is shown in Fig. 2. This compares to the experimental data of Ref. 2 with (1) keeping only the impulse approximation, (2) keeping both single and double, etc. Even with this simple model, the qualitative agreement with the data is remarkable. The magnitude and slope of the primary diffraction peak are well fitted, as is the total cross section (143 mb as against an experimental value of  $152 \pm 8$  mb and the impulse-approximation value of 176 mb). Even more encouraging, the position and magnitude of the first minimum are in very good agreement. The larger-angle data diverge quite drastically from the theoretical prediction. One can now take the somewhat negative attitude that since the Glauber approximation was only justified for small angles, better agreement should not be expected. In Sec. IV we shall take the opposite approach and assume that the theory is valid to larger values of  $q^2$  and ascribe the deviations in Fig. 2 to the poor quality of the nuclear model. Hopefully this enables us to say more about the wave function of  $\text{He}^4$ .

In order to illustrate more features of the multiple-scattering formalism, let us calculate the total nuclear cross section from Eq. (2.21) with the simplification  $\rho=0, \beta^2=0$ :

$$\sigma_N = \frac{2\pi}{\alpha^2} \sum_{j=1}^A \binom{A}{j} \frac{(-1)^{j+1}}{j} \left( \frac{\sigma \alpha^2}{2\pi} \right)^j. \quad (2.22)$$

By differentiating this with respect to  $\sigma$  and then reintegrating, the following representation is obtained:

$$\sigma_N = \frac{2\pi}{\alpha^2} \int_0^\sigma \frac{d\sigma'}{\sigma'} \left[ 1 - \left( 1 - \frac{\sigma' \alpha^2}{2\pi} \right)^A \right]. \quad (2.23)$$

Consider now the limit of a large nucleus for which the number of nucleons  $A$  tends to infinity but at constant density

$$A = c/\alpha^3. \quad (2.24)$$

Then roughly

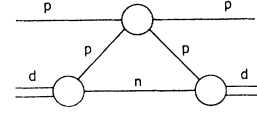
$$\sigma_N \approx \frac{2\pi A^{2/3}}{c} \int_0^\sigma \frac{d\sigma'}{\sigma'} \left[ 1 - \exp\left( -\frac{c\sigma' A^{1/3}}{2\pi} \right) \right]. \quad (2.25)$$

This can be approximated by

$$\sigma_N \approx \frac{2\pi A^{2/3}}{c} \ln \left( 1 + \frac{c\sigma A^{1/3}}{2\pi} \right). \quad (2.26)$$

For very small  $\sigma$  the logarithm can be expanded and the impulse result recovered, where the nuclear cross section is proportional to  $A$ , the number of nucleons.

FIG. 3. Graphical representation of the impulse approximation to elastic proton-deuteron scattering.



For larger  $\sigma$  or  $A$  the cross section is proportional to  $A^{2/3}$ , as common sense tells us it must be. The presence of an extra logarithmic factor is due to the lack of saturation of the Gaussian density. For a uniform density of range  $R$  the logarithm is absent.<sup>11</sup>

### III. DIAGRAMMATIC FORMULATION OF GLAUBER THEORY

In order to illustrate the approximations that were made in Sec. II and in the hope of improving upon them, it is instructive to have a diagrammatic derivation of the theory. Such a derivation has already been given for the specific case of a deuterium nucleus,<sup>12</sup> but the extension to more complicated nuclei appears to involve merely tedious algebra.

Consider first the impulse approximation to proton-deuteron elastic scattering. The deuteron virtually dissociates into a neutron-proton pair, the two protons scatter, and the deuteron is reformed. This is illustrated in Fig. 3. There will, of course, be a similar contribution with the roles of the proton and neutron in the deuteron reversed. The crucial point now is that if Fig. 3 is interpreted as a Feynman graph, then in a certain approximation it can be calculated and leads to the same result that can be found in one of Glauber's papers. Following Ref. 12, we write the amplitude as a four-dimensional Feynman integral. This is most conveniently calculated in the Breit frame where the deuteron momenta before and after the scattering are  $(-+/2)^{1/2}$  and  $-(-+/2)^{1/2}$ . Note that in this system, as in the c.m. frame, we have the relation

$$\mathbf{q}^2 = -t. \quad (3.1)$$

Provided that  $q$  is small compared to the mass of the nucleus, we can then forget the Lorentz contraction and still treat the nucleus as spherically symmetric (neglecting the small  $d$ -state admixture in the deuteron). It is in the spirit of the Glauber theory that while the two protons are interacting, the neutron is completely unaffected. Remember the lens analogy. We therefore replace the neutron propagator associated with the neutron of Fig. 3 by a delta function. In the simple case where all the nucleon spins are ignored, this leads to an amplitude

$$f_{pd}(\mathbf{q}) = \int d^3\mathbf{q}' f_{pp}(\mathbf{q}) \varphi^*(\mathbf{q}' - \frac{1}{4}\mathbf{q}) \varphi(\mathbf{q}' + \frac{1}{4}\mathbf{q}), \quad (3.2)$$

<sup>11</sup> B. M. Udgaonkar and M. Gell-Mann, Phys. Rev. Letters **8**, 346 (1962).

<sup>12</sup> E. S. Abers, H. Burkhardt, V. L. Teplitz, and C. Wilkin, Nuovo Cimento **42**, 365 (1966); Phys. Letters **21**, 339 (1966).

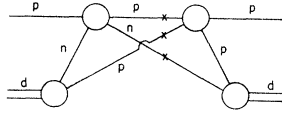


FIG. 4. Graphical representation of the elastic double-scattering contribution to elastic proton-deuteron scattering. In the Glauber approximation, the three particles marked with a cross are taken to be on their mass shells.

where  $\mathbf{q}'$  is the Fermi momentum of the neutron and  $\varphi$  is the deuteron wave function in momentum space. If the spectator neutron is on its mass shell, then obviously the interacting proton can not be. Any off-mass-shell correction is neglected and the physical proton-proton amplitude is fed into the right-hand side of Eq. (3.2). However, this amplitude is required at an energy which is a function of both the incident proton momentum and the Fermi momentum  $\mathbf{q}'$ . In Sec. II the target nucleons were taken as frozen in their positions during the projectile's passage. This corresponds to taking  $f_{pp}(\mathbf{q})$  out of the integration at an energy corresponding to  $q' = 0$ :

$$f_{pd}(\mathbf{q}) = f_{pp}(\mathbf{q}) \int d^3q' \varphi^*(\mathbf{q}' - \frac{1}{4}\mathbf{q}) \varphi(\mathbf{q}' + \frac{1}{4}\mathbf{q}) \equiv f_{pp}(\mathbf{q}) S(\frac{1}{2}\mathbf{q}), \quad (3.3)$$

where  $S$  is the deuteron form factor. This is the same result as we shall obtain later using conventional Glauber theory, Eq. (7.4). The approximation of neglecting the Fermi motion can be very misleading if there is a resonance in the direct channel.<sup>13</sup> Note that the situation does not necessarily get better at higher energies. Disregarding this problem, the relationship between the c.m. energies for  $f_{pp}$  and  $f_{pd}$  in (3.3) is not universal; it has some slight dependence upon  $q$ . This dependence, which is connected with the restriction applying to Eq. (2.7), is very weak for small scattering angles.

A graphical representation also obtains for the re-scattering corrections. In one such term the deuteron dissociates, and the immigrant proton interacts first with the neutron and then with the proton before the deuteron reforms; see Fig. 4.

As before, while one nucleon is interacting the other one is supposed free. A more questionable assumption is that in between the two scatterings, the fast proton also is on its mass shell. This could perhaps be justified if the proton and neutron were far apart compared to the high-energy proton-nucleon force, a situation which is better approximated by the light nuclei, which are

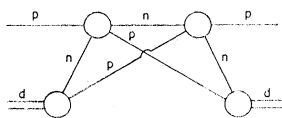


FIG. 5. Graphical representation of the double charge-exchange contribution to elastic proton-deuteron scattering.

<sup>13</sup> R. L. Cool, G. Giacomelli, T. F. Kycia, B. A. Leontic, K. K. Li, A. Lundby, J. Teiger, and C. Wilkin (to be published).

mainly surface, than by the heavier ones. After replacing the three propagators by delta functions and neglecting the Fermi motion, the results of Sec. II are reproduced.

A diagram which is very similar to that of Fig. 4 is that shown in Fig. 5. Here both nucleon-scattering amplitudes involve charge exchange,<sup>14</sup> a possibility which was implicitly neglected in the simple derivation of Sec. II. However, the amplitude associated with Fig. 5 is simply related to that of Fig. 4 by isospin considerations. If the latter amplitude is proportional to  $f_{pn}^{el} f_{pp}^{el}$ , then the former goes as  $-(f_{pn}^{c.e.})^2$ , the minus sign arising from the interchange of an  $n$ - $p$  pair at a deuteron vertex. Since there is only one graph of the charge-exchange type, but two purely elastic ones, a simple prescription to take account of isospin is to make the following replacement in the double-scattering amplitude as calculated in Secs. II or VII:

$$f_{pp} f_{pn} \rightarrow f_{pp} f_{pn} - \frac{1}{2} (f_{pn}^{c.e.})^2 \equiv f_{pp} f_{pn} - \frac{1}{2} (f_{pp} - f_{pn})^2. \quad (3.4)$$

Since charge exchange becomes quite small at high energies, the additional term is not large and can probably be neglected entirely above about 2 GeV/c. Note that expression (3.4) is true only for protons on deuterium, but the techniques can be extended to other systems. The corrected formula for  $p$ -He<sup>4</sup> will be used in Sec. IV.

Similar considerations also apply to coherent double spin flip. In contrast to isospin, at these energies one has very little idea of the spin structure of the nucleon-nucleon amplitude, so that no simple expression like (3.4) can be written down.

We should like to stress that the ability to describe spin and charge degrees of freedom is not the privilege solely of the diagrammatic formulation; the ordinary eikonal method can be generalized to many channels to include them.<sup>15</sup> But the former is much easier to apply.

One place where diagrams seem essential is where there is a truly inelastic intermediate state, such as the  $N^*$  contribution of Fig. 6. There are two big problems about calculating such contributions: the phase of the  $pp \rightarrow pN^*$  amplitude is unknown, and the kinematics resulting from an  $N^*$  mass different from that of the proton is much more complicated. This mass difference introduces a minimum momentum transfer in the  $pp \rightarrow pN^*$  reaction,

$$q_{\min} = (M_{N^*}^2 - m^2)/2k. \quad (3.5)$$

Inserting the mass of the 3-3 resonance, it can be seen

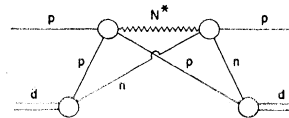


FIG. 6. Graphical representation of a truly inelastic double-scattering contribution to elastic proton-deuteron scattering.

<sup>14</sup> C. Wilkin, Phys. Rev. Letters **17**, 561 (1967).

<sup>15</sup> R. J. Glauber and V. Franco, Phys. Rev. **156**, 1685 (1967).

that this restriction severely cuts down the  $N^*$  contribution at smaller angles; the probability of two relatively large scatterings canceling is very small. The problem of larger angles, say,  $q \sim 2q_{\min}$  or even backward scattering remains unsolved.

The principal result of this section is, hopefully, a clarification of the Glauber approach, especially with regard to charge and spin variables. There is also a series of cautions about the use of the model, especially away from  $t=0$ . In this context it is interesting to note that a Regge behavior of the nucleon amplitudes is incompatible with Glauber's theory.<sup>12</sup> As the energy rises, the effective size of the target proton increases in a Regge model, so that at some point the approximation of putting the fast proton on its mass shell breaks down.

In the main, these problems will be neglected in the applications of the succeeding sections. They should, however, be borne in mind in assessing the value of any results obtained.

#### IV. PROTON-He<sup>4</sup> SCATTERING

In this section we shall endeavor to improve upon the results for  $p$ -He<sup>4</sup> scattering shown in Fig. 2. We first study the nucleon-nucleon amplitude. Shown in Fig. 7 are the data of the Brookhaven group<sup>2</sup> for proton-proton elastic scattering at 1 BeV. As can be seen, a straight line on this semilogarithmic plot fits the data very well indeed out to  $t = -0.45$  (BeV/c)<sup>2</sup>. If the cross section is represented as

$$d\sigma/d\Omega = e^{-\beta^2|t|}, \quad (4.1)$$

then  $\beta^2 = 5.45$  (BeV/c)<sup>-2</sup>. A generalization of this representation to include terms quadratic in  $t$  in the exponent is often to be found in the literature. A minimization routine then leads to a cross section proportional to

$$d\sigma/d\Omega \sim \exp(-\beta^2|t| + \gamma^2 t^2), \quad (4.2)$$

with  $\beta^2 = 6.67$  (BeV/c)<sup>-2</sup>,  $\gamma^2 = 2.64$  (BeV/c)<sup>-4</sup>. The difference between the two forms is not very great (see Fig. 7) until quite large values of  $t$ , for which Glauber's theory is of doubtful use. A more plausible description of the data than (4.2) would take account of the symmetry of the proton-proton cross section about 90° in the c.m. frame.

Both the linear and quadratic forms when extrapolated to  $t=0$  lie above the optical point, the former by 8%, the latter by 17%. On the other hand, the forward-dispersion relations predict that the relative real part of the amplitude  $\rho \sim -0.05 \pm 0.1$ , so that curves should pass extremely close to the optical point. However, the Brookhaven data have quoted errors in the absolute normalization of  $\pm 10\%$ . The above value of  $\rho$  is in good agreement with an evaluation of the Coulomb-nuclear interference effect in a recent proton-proton small-angle scattering experiment.<sup>16</sup> For sim-

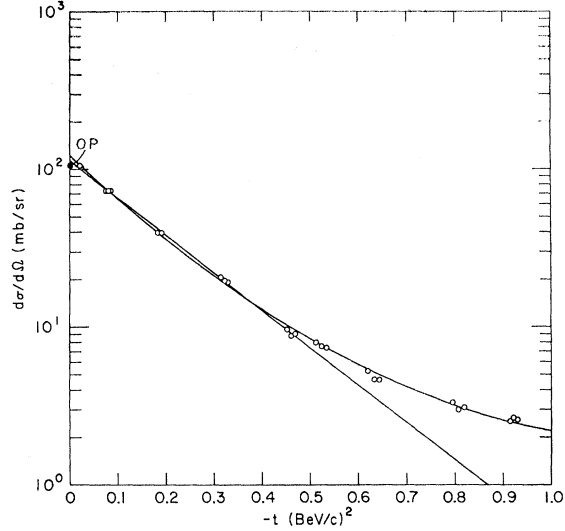


FIG. 7. Forward-angle elastic proton-proton cross section at 1 BeV. The experimental points of Ref. 2 are approximated by the linear and quadratic forms of Eqs. (4.1) and (4.2), respectively.

plicity then we take

$$f_{pp}(t) = (ik\sigma_p/4\pi)(1 - i\rho_p)e^{-\beta^2|t|^{1/2}}, \quad (4.3)$$

with<sup>17</sup>  $\sigma_p = 47.5$  mb,  $\beta^2 = 5.45$  (BeV/c)<sup>-2</sup>,  $\rho_p = -0.05$ . The size of this last parameter is consistent with a Coulomb-nuclear interference measurement.<sup>17</sup> It is, of course, by no means certain that  $\rho$  is independent of angle, but the introduction of too many parameters reduces the theory to the level of curve fitting. In the absence of any experimental evidence to the contrary, we shall take  $\beta^2$  the same for proton-neutron as for proton-proton, but use different estimates for  $\sigma$  and  $\rho$ .

$$f_{pn}(t) = (ik\sigma_n/4\pi)(1 - i\rho_n)e^{-\beta^2|t|^{1/2}}, \quad (4.4)$$

with  $\sigma_n = 40.4$  mb,  $\beta^2 = 5.45$  (BeV/c)<sup>-2</sup>,  $\rho_n = -0.5$ . A value for  $\rho_n$  can be deduced from dispersion relations,<sup>18</sup> or equally indirectly by analyzing small-angle proton-deuteron scattering.<sup>16</sup> Both methods yield  $\rho_n \sim -0.5 \pm 0.15$ , which is consistent with the forward neutron-proton charge-exchange data.<sup>19</sup> Using this value of  $\rho_n$ ,  $\sigma_n$  can be deduced from the proton-deuteron total cross section, as will be discussed in Sec. VIII. We take  $\sigma_{pd} = 83.04 \pm 0.06$  mb, where only the statistical error is quoted.

These parametrizations of the nucleon amplitudes can be used in the description of the helium data. Keeping the same simple nuclear model as in Sec. II, represented by the density function (2.16) and (2.17), we can also take account of multiple-charge-exchange effects. However, any improvement on the predictions shown in Fig. 2 is at best marginal. The discrepancy is largest

<sup>17</sup> D. V. Bugg *et al.*, Phys. Rev. **146**, 980 (1966).

<sup>18</sup> D. V. Bugg and A. A. Carter, Phys. Letters **20**, 203 (1966).

<sup>19</sup> J. L. Friedes *et al.*, Phys. Rev. Letters **15**, 38 (1965).

<sup>16</sup> L. M. C. Dutton *et al.*, Phys. Letters **25B**, 245 (1967).

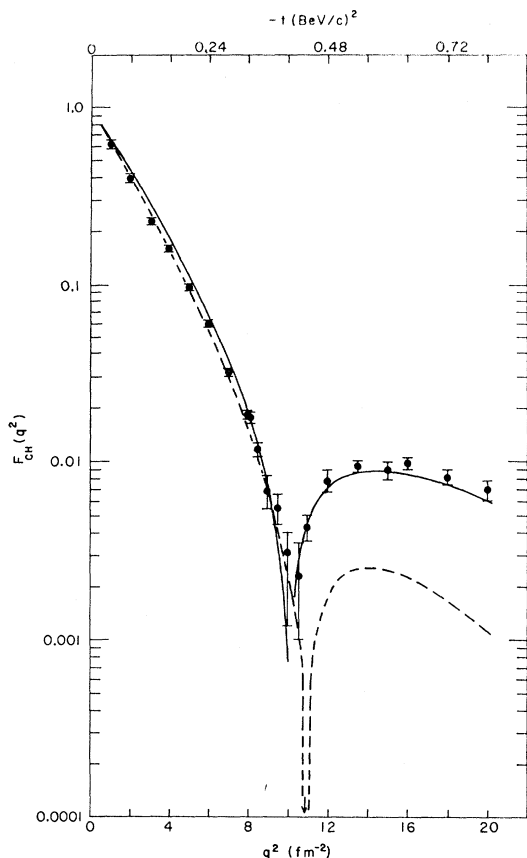


FIG. 8. Elastic electron-He<sup>4</sup> form factor; the experimental data are from Ref. 21. The solid curve is evaluated using the double-Gaussian density (4.11) with  $\alpha^2=0.579 \text{ F}^{-2}$ ,  $\gamma^2=0.308$ , and  $D=0.858$ . Introducing a correlation via Eq. (4.10) with  $C=1$ ,  $\alpha^2=0.573 \text{ F}^{-2}$ , and  $\delta^2=1.552 \text{ F}^{-2}$  leads to the dashed curve.

in the height of the subsidiary maximum; no reasonable variation of the parameters could remove the factor of 2 between theory and experiment. This discrepancy could perhaps be due to the neglected spin-dependent parts of the nucleon-nucleon amplitude. As we have discussed previously, spin-dependence involves the invocation of four additional independent complex functions. Therefore, it seems worthwhile to ignore these and explore the consequences of refining the nuclear model for He<sup>4</sup>. Examination of Fig. 2 shows that the height of the subsidiary maximum is overestimated if triple scattering is neglected, but underestimated if it is included. Provided that we can change the nuclear density to reduce somewhat the double scattering but reduce even more the triple, then a better fit would obtain. Since the multiple-scattering development is roughly an expansion in  $\sigma(r_{ij}^{-2})$ , where  $r_{ij}$  is the distance between two of the nucleons in the nucleus, we can get the required effect if we increase the average nucleon separation in the nucleus. There is one extra piece of information. The electron-scattering results for small  $q^2$  were consistent with a Gaussian shape for the

density function.<sup>20</sup> However, recent experiments at Stanford<sup>21</sup> have now found a sharp minimum in the form factor for  $q^2 \sim 10 \text{ F}^{-2}$ , which is clearly at variance with a Gaussian form (see Fig. 8). A plausible hypothesis, which might explain both the proton and electron results, is that the simple product density (2.16) has to be modified to forbid the close approach of any two of the nucleons in the nucleus. This nucleon hard core can be introduced into the density function via a Jastrow correlation function  $g(r_{ij})$ ,

$$\rho_J(\mathbf{r}_1, \dots, \mathbf{r}_4) = \prod_j \bar{\rho}(\mathbf{r}_j) \prod_{i \leq j} [1 - g(|\mathbf{r}_i - \mathbf{r}_j|)] \quad (4.5)$$

with the subsidiary conditions

$$g(r) \rightarrow 0 \quad \text{as } r \rightarrow \infty; \quad (4.6)$$

if the core is really hard, then

$$g(0) = 1. \quad (4.7)$$

Since for small  $q^2$  the electron data are consistent with a Gaussian density, we can, as before, try

$$\bar{\rho}(\mathbf{r}_i) = e^{-\alpha^2 r_i^2} \quad (4.8)$$

and ascribe all the deviations of the charge density to the Jastrow function  $g$ . This is, however, an assumption and if, for example, it reproduces the Stanford data it is not in itself evidence for a correlation. Since it is doubtful whether the experiments, as yet, are very sensitive to the shape of  $g$ , for computational simplicity we take

$$g(r_{ij}) = C e^{-\delta^2 r_{ij}^2}, \quad (4.9)$$

where  $C=1$  for a hard core. The distribution then becomes

$$\rho_J(\mathbf{r}_1, \dots, \mathbf{r}_4) = N \prod_j e^{-\alpha^2 r_j^2} \prod_{i \leq j} [1 - C \exp(-\delta^2 r_{ij}^2)]. \quad (4.10)$$

To check whether the data are really dependent upon a correlation, it is important to try to interpret the experiments by modifying only the single-particle densities and dropping the correlation. Now if the nucleon-nucleon hard core is of long range, we might expect that this would result in some decrease of density in the middle of the  $\alpha$  particle. Four strongly attractive billiard balls have a tetrahedron as their lowest energy state and this has zero density in the middle. Therefore, we want to reduce  $\bar{\rho}(r)$  for small  $r$ . An example of this type of model is

$$\rho_{DG}(\mathbf{r}_1, \dots, \mathbf{r}_4) = N \prod_j \exp(-\alpha^2 r_j^2) [1 - D \exp(-\alpha^2 r_j^2 / \gamma^2)]. \quad (4.11)$$

<sup>20</sup> G. R. Bureson and H. W. Kendall, Nucl. Phys. **19**, 68 (1960).

<sup>21</sup> R. F. Frosch, J. S. McCarthy, R. E. Rand, and M. R. Yearian, Phys. Rev. **160**, 874 (1967).

One can, of course, study even more complicated forms, since it is by no means certain that a three-parameter function such as (4.10) or (4.11) can reproduce all the aspects of the two sets of data. Taking the direct product we have

$$\begin{aligned} \rho_{\text{DGJ}}(\mathbf{r}_1, \dots, \mathbf{r}_4) \\ = N \prod_j \exp(-\alpha^2 r_j^2) [1 - D \exp(-\alpha^2 r_j^2 / \gamma^2)] \\ \times \prod_{j < i} [1 - C \exp(-\delta^2 r_{ij}^2)]. \quad (4.12) \end{aligned}$$

When the density functions are as complicated as these, the Gartenhaus-Schwartz transformation<sup>8</sup> is not a simplification and it is easier to deal with the c.m.  $\delta$  function explicitly. We first rearrange the basic equation (2.13) so that the integration over the nuclear coordinates can be performed last. The other integrations can be performed analytically and lead to

$$\begin{aligned} F(q) = \int d^3 r_1 \dots d^3 r_4 \rho(\mathbf{r}_1, \dots, \mathbf{r}_4) \delta^{(3)}(\mathbf{r}_1 + \dots + \mathbf{r}_4) \\ \times [F_1 + F_2 + F_3 + F_4], \quad (4.13) \end{aligned}$$

where  $F_1$ ,  $F_2$ ,  $F_3$ , and  $F_4$  are the contributions of single, double, etc., scattering. In closed form they are

$$F_1 = (ik/2\pi)(f_p + f_n) e^{i\mathbf{q} \cdot \mathbf{s}_1} e^{-\beta^2 q^2 / 2}, \quad (4.14a)$$

$$\begin{aligned} F_2 = - (3ik/16\pi^2 \beta^2) f_p f_n e^{i(\mathbf{q}/2) \cdot (\mathbf{s}_1 + \mathbf{s}_2)} \\ \times e^{-\beta^2 q^2 / 4} e^{-(\mathbf{s}_1 - \mathbf{s}_2)^2 / 4\beta^2}, \quad (4.14b) \end{aligned}$$

$$\begin{aligned} F_3 = \frac{ik f_p f_n (4 f_p f_n - f_p^2 - f_n^2)}{192\pi^3 \beta^4} e^{i(\mathbf{q}/3) \cdot (\mathbf{s}_1 + \mathbf{s}_2 + \mathbf{s}_3)} e^{-\beta^2 q^2 / 6} \\ \times \exp\left\{-\left[\frac{1}{3}(s_1^2 + s_2^2 + s_3^2) - \frac{1}{3}(s_1 + s_2 + s_3)^2\right] / 2\beta^2\right\}, \quad (4.14c) \end{aligned}$$

$$\begin{aligned} F_4 = - \frac{ik [f_p^2 f_n^2 - f_p f_n (f_p - f_n)^2]}{1024\pi^4 \beta^6} \\ \times \exp\left\{-\left[(s_1 + s_2 + s_3)^2 + (s_1^2 + s_2^2 + s_3^2)\right] / 2\beta^2\right\} \\ \times \exp(-\frac{1}{8}\beta^2 q^2), \quad (4.14d) \end{aligned}$$

where we have used the abbreviation  $f = \sigma(1 - i\rho)$ . In evaluating  $F_4$ , the  $s_4$  coordinate has been eliminated by the  $\delta$  function. Multiple charge-exchange effects which are included in (4.14) are examined for this case in Appendix A.

After having performed the integration over the  $r_4$  coordinate with the  $\delta$  function, all the density functions considered were sums of terms of the form

$$\rho \sim \exp(-a_{ij}^{(3)} r_i r_j), \quad i, j = 1, 2, 3 \quad (4.15)$$

where  $A^{(3)} = (a_{ij}^{(3)})$  is a real symmetric  $3 \times 3$  matrix. Moreover, all the operators  $F_m$  have the representation

$$F \sim \exp[-(\mathbf{s}_1, \mathbf{s}_2, \mathbf{s}_3, i\mathbf{q}) B^{(4)} (\mathbf{s}_1, \mathbf{s}_2, \mathbf{s}_3, i\mathbf{q})^T], \quad (4.16)$$

with  $B^{(4)}$  a real symmetric  $4 \times 4$  matrix. If we define  $B^{(3)}$  to be the north-west submatrix of  $B^{(4)}$  and  $A^{(4)}$  to be the matrix  $A^{(3)}$  extended to  $4 \times 4$  by the addition of a null fourth column and row, then it is shown in Appendix B that

$$\begin{aligned} \int F \rho d^3 r_1 d^3 r_2 d^3 r_3 = \frac{(\pi^{3/2})^3}{\|A^{(3)}\|^{1/2} \|A^{(3)} + B^{(3)}\|} \\ \times \exp\left(+q^2 \frac{\|A^{(4)} + B^{(4)}\|}{\|A^{(3)} + B^{(3)}\|}\right). \quad (4.17) \end{aligned}$$

The calculation of the amplitude from (4.13) principally involves sums of integrals like the above. In the worst case (4.12) there are 4096 terms. All that is required, however, is bookkeeping and this is best left to the computer.

In Fig. 8 the results of the recent electron scattering measurements from Stanford are shown. As was stressed before, these data are sensitive only to the impulse approximation (2.14), so that the plotted form factor is the Fourier transform of the charge distribution except in the vicinity of the diffraction minimum ( $q^2 \sim 10 \text{ F}^{-2}$ ), where higher-order electromagnetic corrections fill in the potential zero. To account for the finite proton size, we have taken the electromagnetic form factor of the proton as the by now conventional double pole<sup>22</sup>

$$G(q) = (1 + q^2/a^2)^{-2}, \quad (4.18)$$

where  $a = 0.71 \text{ BeV}/c$ .

Let us first consider the predictions of the double-Gaussian density (4.11). There are three parameters to be determined here, viz.,  $\alpha$ ,  $\gamma$ , and  $D$ . This was done by a simultaneous least-squares fit to both the electron and proton cross sections. Since the Glauber approximation is of doubtful validity for large-angle proton scattering, and the impulse approximation does not hold near the electron minimum, such experimental points were eliminated in the fitting process. The outcome of this procedure is shown in Fig. 8 for electrons and in Fig. 9 for protons with  $\alpha^2 = 0.579 \text{ F}^{-2}$ ,  $\gamma^2 = 0.308$ , and  $D = 0.858$ . The agreement with the proton data is markedly better than that of the simple model (Fig. 2), especially in the region of the subsidiary maximum. In addition, the electron scattering form factor of Fig. 9 is quite well reproduced, in particular the position of the minimum and the height of the maximum.

We now turn to the other limit and try to ascribe the discrepancies of the simple model with experiment to a correlation function rather than to the single-particle density. Constraining  $C$  to unity in model (4.10), the minimization routine leads to values  $\alpha^2 = 0.573 \text{ F}^{-2}$  and  $\delta^2 = 1.552 \text{ F}^{-2}$ , i.e., a quite acceptable healing distance of the order of 0.8 F. However, the improvement in the proton predictions (Fig. 9) over those of the simple

<sup>22</sup> M. Goitein, J. R. Dunning, and R. Wilson, Phys. Rev. Letters 18, 1018 (1967).

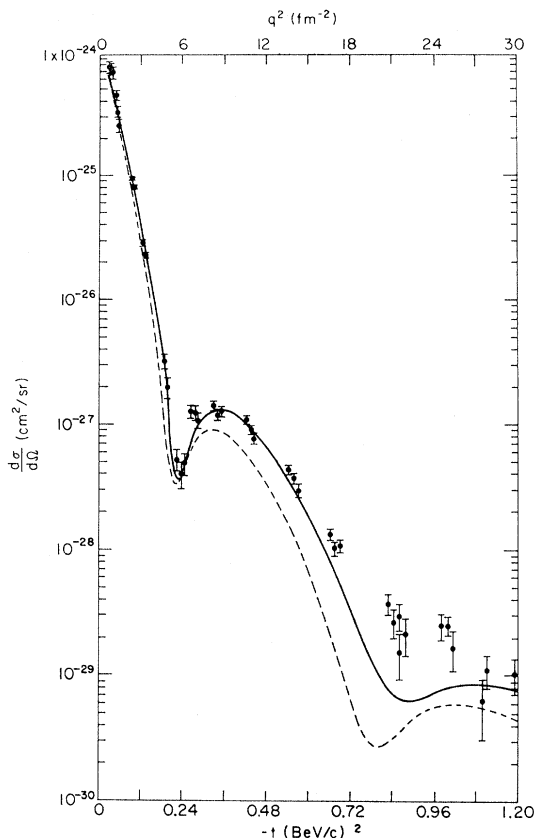


FIG. 9. Elastic proton- $\text{He}^4$  cross section at 1 BeV; the experimental data are from Ref. 2. The solid curve is evaluated using the double-Gaussian density (4.11) with  $\alpha^2=0.579 \text{ F}^{-2}$ ,  $\gamma^2=0.308$ , and  $D=0.858$ . Introducing a correlation via Eq. (4.10) with  $C=1$ ,  $\alpha^2=0.573 \text{ F}^{-2}$ , and  $\delta^2=1.552 \text{ F}^{-2}$  leads to the dashed curve.

Gaussian model (Fig. 2) is very small. The electron scattering minimum is in about the right position, but this is not surprising since this carries great weight in the fitting routine. Nevertheless the predicted maximum is a factor of 4 too low. If  $C$  is taken less than 1, then this maximum is depressed even further.

To see the effect of varying both the single-particle density and the correlation function, density (4.12) was considered. Putting  $C=1$ , the other parameters were determined to be  $\alpha^2=0.644 \text{ F}^{-2}$ ,  $\delta^2=6.0 \text{ F}^{-2}$ ,  $\gamma^2=0.190$ , and  $D=1$ . Despite the good over-all agreement with both the electron data of Fig. 10 and proton data of Fig. 11, the amelioration over the no-correlation case (4.11) is not too large, except in the value of the form factor for small  $q^2$ . This manifested itself in the minimization routine by the relative insensitivity of the data to a simultaneous increase of  $\gamma$  and  $\delta$  from the above values, subject to the condition that the electron minimum be kept in the correct region.

What then have we learned from the electron and proton experiments? In the present state of theory and experiment, there seems to be no positive evidence for nucleon-nucleon correlations in  $\text{He}^4$ . Only a slightly

better agreement with experiment is obtained by the inclusion of a correlation which we know must be present, viz., the hard core. It is, however, likely that similar amelioration would result if the extra parameters were absorbed in the single-particle density rather than in the Jastrow function. Of course we do not know with what precision the Glauber theory should work, especially when spin effects are neglected. Somewhat

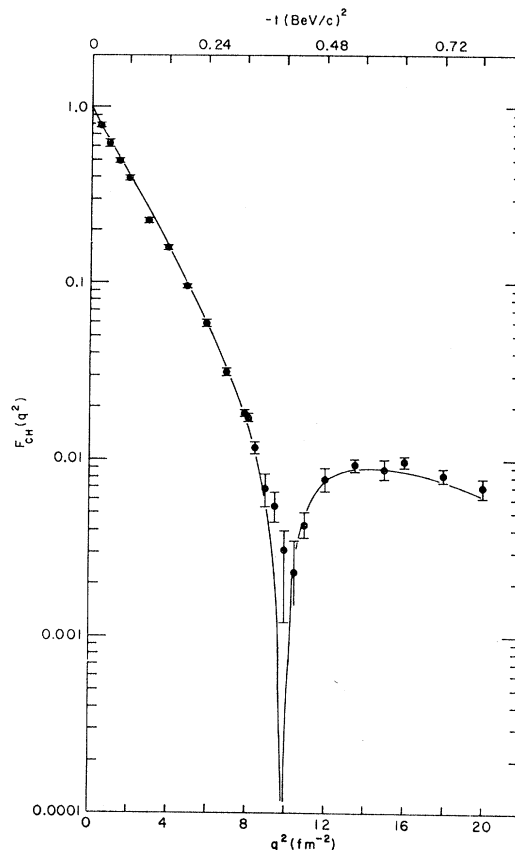


FIG. 10. Elastic electron- $\text{He}^4$  form factor; the experimental data are from Ref. 21. The theoretical curve is derived using a density (4.12) containing the double-Gaussian and a correlation with  $C=1$ ,  $D=1$ ,  $\alpha^2=0.644 \text{ F}^{-2}$ ,  $\delta^2=6.0 \text{ F}^{-2}$ , and  $\gamma^2=0.190$ .

similar conclusions were reached by Cys $\acute{z}$  and Le $\acute{s}$ niak,<sup>23</sup> who work in a much cruder mathematical framework, neglecting both the c.m.  $\delta$  function and the finite proton size.

An objection which may be, and frequently has been, raised by nuclear theorists is that density (4.12) with  $D=1$  is zero at the origin and this is unphysical. The four-billiard-ball model would be vitiated by the zero-point motion. We have no reply to this argument except to say that this particular model does not, in fact, suppose an actual hole in the middle of  $\text{He}^4$ . In Fig. 12 is plotted the density obtained by integrating over the three unwanted coordinates of Eq. (4.12). With the

<sup>23</sup> W. Cys $\acute{z}$  and L. Le $\acute{s}$ niak, Phys. Letters **25B**, 319 (1967).

same parameters that gave the best fits of Figs. 11 and 12, this density is zero for  $r=0$ . However, this is only the density of nucleon centers and the central depression is completely eliminated by folding in the finite proton size. It is really this resultant matter density with which intuition is usually concerned. The density normally quoted in the literature is the charge density, and it may well be if the one-particle density  $\tilde{\rho}$  were derived from this it would have similar unpleasant features.

### V. SCATTERING FROM $p$ -SHELL NUCLEI: OXYGEN AND CARBON

It was shown many years ago that elastic electron scattering from the nuclei  $C^{12}$  and  $O^{16}$  can be very well

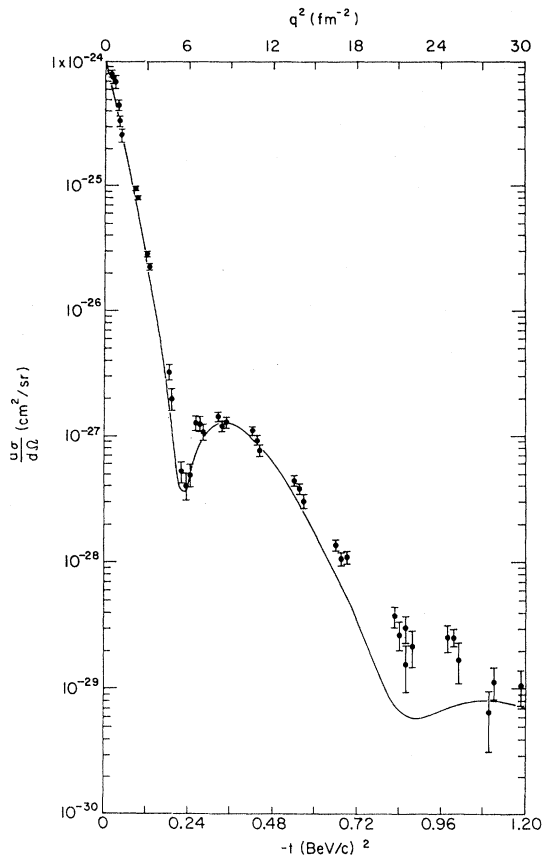


FIG. 11. Elastic proton- $He^4$  cross section at 1 BeV; the experimental data are from Ref. 2. The theoretical curve is derived using a density (4.12) containing the double-Gaussian and a correlation with  $C=1$ ,  $D=1$ ,  $\alpha^2=0.644 \text{ F}^{-2}$ ,  $\delta^2=6.0 \text{ F}^{-2}$ , and  $\gamma^2=0.190$ .

represented in terms of the shell model with harmonic-oscillator wave functions.<sup>24</sup> As was emphasized in Sec. II, these functions are extremely expedient in that the c.m.  $\delta$  function can be disposed of via the Gartenhaus-Schwartz transformation.<sup>8</sup> In the case of  $He^4$ , because

<sup>24</sup> H. F. Ehrenberg *et al.*, Phys. Rev. **113**, 666 (1959).

of charge and spin variables, the four target nucleons are distinguishable; for the  $p$ -shell nuclei they are not, and so we must expect effects here from the Pauli principle. However, there will be no important effects in electron scattering since in the Born approximation use is made only of a one-body operator. We first then try a simple product wave function with four particles in  $s$  states and  $A-4$  in  $p$  states, which, as was explained above, agrees with the electron data

$$\rho(\mathbf{r}_1, \dots, \mathbf{r}_A) = \prod_{j=1}^4 \tilde{\rho}_s(\mathbf{r}_j) \prod_{j=5}^A \tilde{\rho}_p(\mathbf{r}_j), \quad (5.1)$$

where the  $s$ - and  $p$ -wave densities are

$$\rho_s(\mathbf{r}) = (\alpha^2/\pi)^{3/2} e^{-\alpha^2 r^2}, \quad (5.2)$$

$$\rho_p(\mathbf{r}) = (2\alpha^5/3\pi^{3/2}) r^2 e^{-\alpha^2 r^2}. \quad (5.3)$$

If this density is substituted into the basic Eq. (2.13), after removing the  $\delta$  function, one gets

$$F(q) = \left( \frac{ik}{2\pi} \right) e^{q^2/4A\alpha^2} \int e^{iq \cdot \mathbf{b}} d^{(2)}\mathbf{b} \int d^{(3)}\mathbf{r}_1 \dots d^{(3)}\mathbf{r}_A \\ \times \prod_{j=1}^4 \rho_s(\mathbf{r}_j) \prod_{j=5}^A \rho_p(\mathbf{r}_j) \\ \times \left[ 1 - \prod_{i=1}^A \left( 1 - \frac{\sigma(1-i\rho)}{4\pi\beta^2} e^{-(b-s_i)^2/2\beta^2} \right) \right]. \quad (5.4)$$

Note that in this expression the proton-proton and

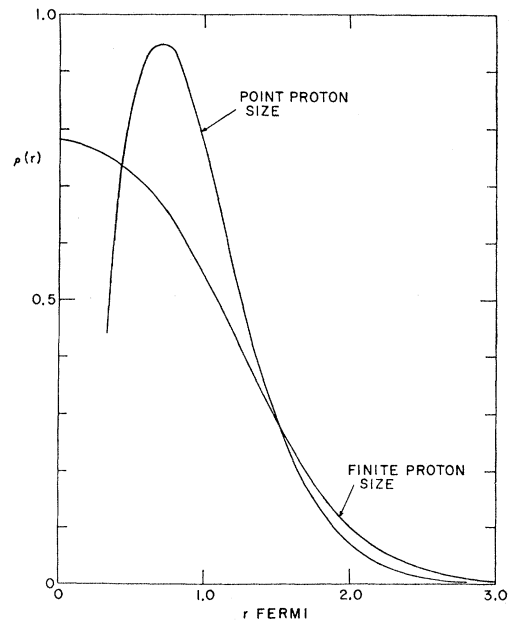


FIG. 12. Matter density of  $He^4$  corresponding to the best fits of Figs. 10 and 11. The central depression associated with the point proton size is completely eliminated when the finite proton size is folded in.

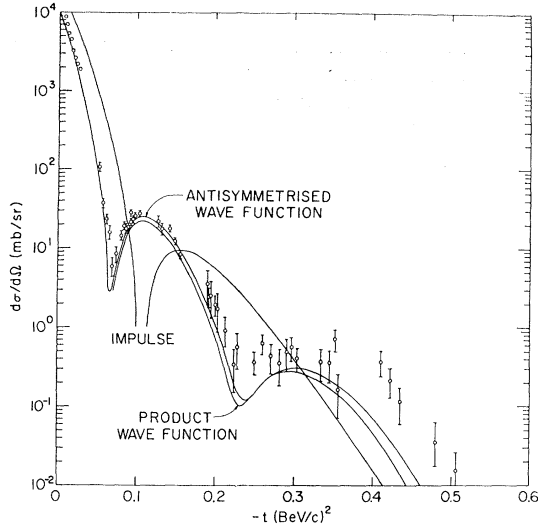


FIG. 13. Elastic proton- $O^{16}$  cross section at 1 BeV; the experimental data are from Ref. 2. The theoretical curves are evaluated with  $\sigma = 44$  mb,  $\rho = -0.275$ ,  $\beta^2 = 5.45$  (BeV/c) $^2$ , and  $\alpha^2 = 0.342$  F $^{-2}$ . The effect of using an antisymmetrized nuclear wave function rather than a simple product is shown. These are to be compared with the impulse approximation which characterizes reasonably the electron scattering results.

proton-neutron amplitudes have been replaced by some average nucleon amplitude. The evaluation of charge-exchange effects, though straightforward, is tedious in a nucleus as large as carbon and does not fit in well with the numerical techniques which we shall employ. Without charge exchange, keeping the individual proton and neutron amplitudes has not much point.

Since the  $r_j$  integrations are now separable,  $F$  can be reduced to a single Fourier transform

$$F(q) = \left(\frac{ik}{2\pi}\right) e^{q^2/4A\alpha^2} \int e^{iq \cdot b} d^2(b) b \times \left\{ 1 - \left[ 1 - \frac{\sigma(1-i\rho)}{4\pi} \left( \frac{2\alpha^2}{1+2\alpha^2\beta^2} \right) e^{-\alpha^2 b^2/(1+2\alpha^2\beta^2)} \right]^4 \right. \\ \times \left[ 1 - \frac{\sigma(1-i\rho)}{2\pi} \left( \frac{\alpha^2}{1+2\alpha^2\beta^2} - \frac{2\alpha^2}{3(1+2\alpha^2\beta^2)^2} + \frac{2\alpha^4 b^2}{3(1+2\alpha^2\beta^2)^3} \right) e^{-\alpha^2 b^2/(1+2\alpha^2\beta^2)} \right]^{A-4} \left. \right\}. \quad (5.5)$$

Now in the simple  $s$ -wave model of the nucleus studied in Sec. II, the integrand was expanded in a polynomial in  $\sigma$ , the transform performed analytically, and the result presented in a simple form. The same approach can be used for Eq. (5.5) except that the final result is by no means simple.

The assumption that the nuclei are spherical has led to an integrand which depends only on the magnitude

of  $b$ , viz., it is of the form

$$F(q) = ik \int_0^\infty b db J_0(qb) \langle \Gamma_N(b) \rangle. \quad (5.6)$$

The integration can now be performed numerically, so that all the multiple scatterings are taken into account simultaneously. The numerical integration routine<sup>25</sup> used reproduced known functions with an accuracy of 1 part in  $10^7$ . This is critical in order to reproduce well the strong cancellations in the vicinity of the diffraction minima.

The nucleon-nucleon parameters were taken as the average of those used to describe He<sup>4</sup>:  $\sigma = 44.0$  mb,  $\rho = -0.275$ , and  $\beta^2 = 5.45$  (BeV/c) $^2$ . The radius of O<sup>16</sup> as measured by electron scattering<sup>26</sup> is  $\langle r^2 \rangle^{1/2} = 2.65$  F. When due account is taken of the proton form factor and the c.m. motion, this leads to a value of the size parameter  $\alpha^2 = 0.342$  F $^{-2}$ . With these parameters the  $p$ -O<sup>16</sup> elastic amplitude was calculated and is shown in Fig. 13. The agreement over so many orders of magnitude is extremely impressive and lends support to both the scattering theory and the simple nuclear model which we have used. For comparison the impulse approximation is also shown. It bears no clear relation with the data. The predicted total cross (459 mb) accords well with the experimental value (475 ± 44 mb).

As was remarked earlier in this section, a more reasonable nuclear wave function would include the effects of the Pauli principle. In general, it is necessary to include the incident proton in the antisymmetrization, but the effects of this are negligible for small-angle high-energy elastic scattering. Since we are neglecting charge exchange it is sufficient to antisymmetrize the target protons and neutrons separately and forget the correlations between the two groups.

For C<sup>12</sup> we shall take the proton wave function as  $(s^{1/2})^2(p^{3/2})^4$ , and O<sup>16</sup> as  $(s^{1/2})^2(p^{3/2})^4(p^{1/2})^2$ . For a harmonic oscillation the  $s$ - and  $p$ -wave radial wave functions are

$$\begin{aligned} \varphi_s(r) &= (4\alpha^3/\pi^{1/2})^{1/2} e^{-\alpha^2 r^2/2}, \\ \varphi_p(r) &= (8\alpha^5/3\pi^{1/2})^{1/2} r e^{-\alpha^2 r^2/2}. \end{aligned} \quad (5.7)$$

The spin angular functions are

$s$  wave

$$\begin{aligned} |s \frac{1}{2} \frac{1}{2}\rangle &= Y_0^0 u_+, \\ |s \frac{1}{2} -\frac{1}{2}\rangle &= Y_0^0 u_-; \end{aligned} \quad (5.8a)$$

$p_{3/2}$  wave

$$\begin{aligned} |p \frac{3}{2} \frac{3}{2}\rangle &= Y_1^1 u_+, \\ |p \frac{3}{2} \frac{1}{2}\rangle &= (\sqrt{\frac{2}{3}}) Y_1^0 u_+ + \frac{1}{\sqrt{3}} Y_1^1 u_-, \\ |p \frac{3}{2} -\frac{1}{2}\rangle &= \frac{1}{\sqrt{3}} Y_1^{-1} u_+ + (\sqrt{\frac{2}{3}}) Y_1^0 u_-, \\ |p \frac{3}{2} -\frac{3}{2}\rangle &= Y_1^1 u_-; \end{aligned} \quad (5.8b)$$

<sup>25</sup> We are grateful to Dr. R. F. Peierls for supplying us with this numerical routine.

<sup>26</sup> P. Goldhammer, Rev. Mod. Phys. **35**, 40 (1963).

$p_{1/2}$  wave

$$\begin{aligned} |p_{\frac{1}{2}} \frac{1}{2}\rangle &= -\frac{1}{3}\sqrt{3}Y_1^0u_{+} + (\sqrt{\frac{2}{3}})Y_1^1u_{-}, \\ |p_{\frac{1}{2}} -\frac{1}{2}\rangle &= -(\sqrt{\frac{2}{3}})Y_1^{-1}u_{+} + (\sqrt{\frac{1}{3}})Y_1^0u_{-}; \end{aligned} \quad (5.8c)$$

here  $u_{+(-)}$  represents a proton with spin up (down). The spherical harmonics are referred to the coordinate system of Fig. 14, where  $z$  is the direction of the incident proton. Hence

$$\begin{aligned} x_j &= r_j \cos\theta_j, \\ y_j &= r_j \sin\theta_j \cos\varphi_j, \\ z_j &= r_j \sin\theta_j \sin\varphi_j. \end{aligned} \quad (5.9)$$

Since for elastic scattering the amplitude has cylindrical symmetry in  $\mathbf{q}$  and hence in  $\mathbf{b}$ , we can evaluate  $\langle \Gamma_N(\mathbf{b}) \rangle$  by choosing  $\mathbf{b}$  to lie in a specific direction, say along the  $x$  axis. The individual scattering operators become

$\Gamma(\mathbf{b}-\mathbf{s}_j)$

$$\begin{aligned} &= \frac{\sigma_j}{4\pi\beta^2} \exp\left(-\frac{(\mathbf{b}-\mathbf{s}_j)^2}{2\beta^2}\right) \\ &= \frac{\sigma_j}{4\pi\beta^2} \exp\left(-\frac{b^2 - 2bx_j + x_j^2 + y_j^2}{2\beta^2}\right) \\ &= \frac{\sigma_j}{4\pi\beta^2} \exp\left(-\frac{b^2 - 2br_j \cos\theta_j + r^2 - r^2 \sin^2\theta_j \sin^2\varphi_j}{2\beta^2}\right). \end{aligned} \quad (5.10)$$

To complete the treatment, we must antisymmetrize the proton wave functions and this we do by taking the ground-state wave function as a Slater determinant rather than just a simple product:

$$\psi(r_1, \dots, r_Z) = (Z!)^{-1/2} \|\psi_m(r_n)\|, \quad (5.11)$$

where the  $\psi_m$  are the wave functions given by (5.7) and (5.8). We then need matrix elements of the form

$$M = \langle \psi | \Gamma_N | \psi \rangle = I - \langle \psi | O | \psi \rangle, \quad (5.12)$$

where

$$O = \prod_j (1 - \Gamma_j). \quad (5.13)$$

As can be seen in (5.13), the operator  $O$  has the important property that it is factorizable into operators which act in one and only one particle subspace, so that

$$O | \psi \rangle = (Z!)^{-1/2} \|O(n)\psi_m(r_n)\|. \quad (5.14)$$

It is well known that antisymmetrization is only required for the bra, and that we can take the ket as

$$\langle \psi | = (Z!)^{1/2} \|\delta_{mn}\psi_m^\dagger(r_n)\|. \quad (5.15)$$

Combining the above equations

$$\begin{aligned} \langle \psi | \Gamma_N | \psi \rangle &= I - \|\psi_n^\dagger(r_n) O(n) \psi_m(r_n)\| \\ &\equiv I - \|O_{nm}\|, \end{aligned} \quad (5.16)$$

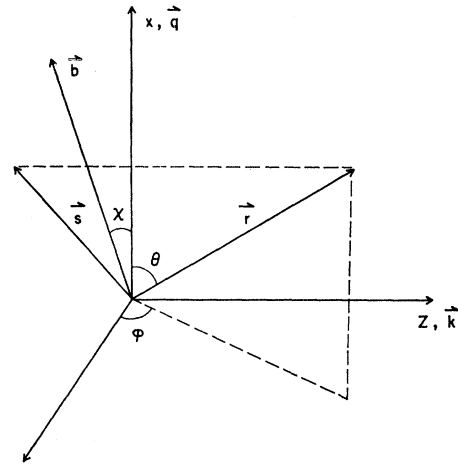


FIG. 14. Coordinate system used for elastic proton-carbon and proton-oxygen scattering.

where the  $O_{nm}$  are matrix elements defined by

$$O_{nm} = \delta_{nm} - \int \psi_m^*(\mathbf{r}) \Gamma(\mathbf{b}-\mathbf{s}) \psi_n(\mathbf{r}) d^3\mathbf{r}. \quad (5.17)$$

Consequently, the effect of antisymmetrizing the wave functions is to replace the integrand of Eq. (5.5) by 1 minus the square of an  $8 \times 8$  determinant. The squaring takes care of all the multiple scatterings of the neutrons, which are assumed identical to the protons. It is straightforward to derive the expression for the matrix  $O$ , which is given in Appendix C. The elements are just linear combinations of  $\omega_i (i=1, \dots, 5)$ , which are polynomials in  $b$  multiplied by an exponential in  $b^2$ . Because of the choice of quantization and  $\mathbf{b}$  axes, the operator  $\Gamma$  of Eq. (5.10) is even in  $\cos\varphi$  and hence can only cause transitions of the type  $\Delta J_x = \text{even}$ . For this reason  $O$  decomposes into two equivalent distinct submatrices, so that the determinant is the square of a function of the  $\omega_i$ :

$$\|O\| = [(1-\omega_1)(1-\omega_3) - \omega_4^2]^2 [(1-\omega_2)^2 - \omega_5^2]^2. \quad (5.18)$$

Now since we have taken the target nucleons as being in a central potential (the same radial wave function is used for the  $p_{3/2}$  states as for the  $p_{1/2}$ ), the expression obtained for  $\|O\|$  in the  $j$ - $j$  representation must be the same as that holding in the  $L$ - $S$  scheme. Things are rather simpler in the latter case because the nucleon-nucleon interaction is assumed to leave  $S$  invariant, and so  $O$  decomposes into four distinct  $2 \times 2$  submatrices.

The appropriate scattering amplitude was calculated as before by a numerical Bessel transform, with the expression (5.18) replacing the simpler integrand of Eq. (5.5). The predicted cross section is exhibited in Fig. 13, where it is compared with both the experimental data and the results obtained from the product wave function. Although it is hard to improve upon the quality of the latter, the antisymmetrized theory does

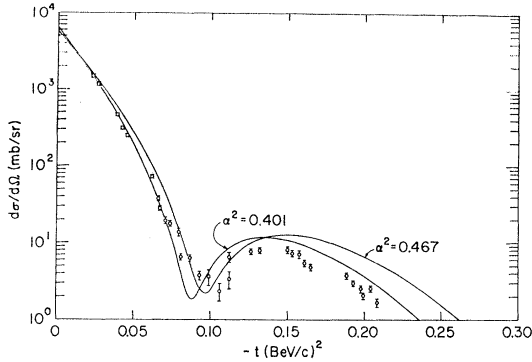


FIG. 15. Elastic proton- $C^{12}$  cross section at 1 BeV; the experimental data are from Ref. 2. The theoretical curves result from a multiple-scattering calculation with antisymmetrized wave functions and  $\sigma=44$  mb,  $\rho=-0.275$ , and  $\beta^2=5.45$  (BeV/c) $^2$ . The dependence upon the carbon radius parameter is illustrated;  $\alpha^2=0.401$  F $^{-2}$  is the value derived from electron scattering. The impulse-approximation minimum occurs at  $t\sim-0.15$  (BeV/c) $^2$ .

fit the data marginally but not significantly better. Throughout the whole range it lies slightly higher, which is owing to the inclusion now of transitions where an  $s$ -wave nucleon is excited to a  $p$  wave, while another nucleon does the opposite transition. The predicted total cross section is 467 mb.

The remarkably good description of the  $O^{16}$  data leads one to believe that the Glauber theory can give numerically meaningful results for this kind of nucleus. We are thus encouraged to investigate  $C^{12}$  which has roughly the same radius, density, etc. Since there are only six protons in  $C^{12}$ , the matrix  $O$  will now only be  $6\times 6$ . This can easily be obtained from the  $8\times 8$  matrix corresponding to  $O^{16}$  [see Eq. (C6)] by deleting the rows and columns associated with the  $p_{1/2}$  states. We then obtain

$$\langle \Gamma_N \rangle = 1 - \|O\|^2, \quad (5.19)$$

with

$$\|O\| = [(1-\omega_1)(1-\omega_2)(1-2\omega_3/3-\frac{1}{3}\omega_2) - \frac{2}{3}\omega_4^2(1-\omega_2) - \frac{1}{3}\omega_5^2(1-\omega_1)]. \quad (5.20)$$

Once more the numerical Bessel transform provides us with the scattering amplitude. Using the same values of the nucleon-nucleon parameters that were so successful in  $O^{16}$  and  $He^4$ , together with  $\alpha^2=0.401$  F $^{-2}$ , which is the size obtained from electron scattering, $^{26}$  the predicted cross section is compared with the Brookhaven points in Fig. 15. Although there is some general qualitative agreement, it is by no means the striking quantitative success that oxygen was. The minimum is expected at too small a value of  $q$  and the data lie 50% below the theory in the vicinity of the subsidiary maximum. If the radius of carbon is decreased so that the minimum occurs in the right region, the problem of the subsidiary maximum is possibly aggravated, as can be seen from the figure.

The contrast between our findings for  $O^{16}$  and  $C^{12}$  leads one to suspect the nuclear model used in the latter

case. There is much evidence to show that  $C^{12}$  is, in fact, a very deformed (oblately) nucleus. The first excited state ( $2^+$  at 4.4 MeV) looks very much like the second member of a rotational band with  $K=0$ . Impulse approximation, which describes well electron scattering, is not sensitive to a deformation since the *single*-particle density is spherically symmetric. Effects can only come in second order, where, say, the first scattering excites the  $2^+$  state and the second leads back to the ground state. Consequently, it is expected that the deformation will manifest itself first around the secondary maximum where double scattering is the most important term. In fact, on the basis of a completely black ellipsoid model, Drozdov $^{27}$  has shown that the height of the subsidiary maximum does decrease as the deformation increases. Although his model is considerably cruder than the one used in this work, it is known that this characteristic is much more general. It may then be possible to deduce the size of the deformation from a careful analysis of the data in this region. Some approaches that are worth trying include the following: (a) In the same spirit as Drozdov, put the nucleons into a deformed oscillator well and neglect the problem that the nucleus will not, in general, then have a well-defined angular momentum—the multiple scatterings are mainly a function of the geometry of the nucleus. (b) Mix in more configurations of the shell model. (c) In order to reduce the number of configurations use the alpha cluster model for  $C^{12}$ —this has an intrinsic deformation built in.

As was remarked in the case of  $He^4$ , the depth of the first diffraction minimum is quite a sensitive function of the real parts of the nucleon-nucleon amplitudes. The curves for  $O^{16}$  in Fig. 13 have the average  $\rho$  about  $\pm 0.3$  (it is independent of the over-all sign), and although this is probably not the optimum value, the agreement gets worse if  $\rho$  is changed by more than 0.1, say.

## VI. INELASTIC SCATTERING FROM $C^{12}$

In the Brookhaven experiments there was only one example of nuclear excitation, where the level could be cleanly separated from both the ground state and the higher excited levels. This was the case of the  $2^+$  (4.4-MeV) state in  $C^{12}$ . As was emphasized in Sec. II, the Glauber approximation should be just as valid for an inelastic process as for the elastic scattering cross section. We should like, therefore, to develop the formalism necessary to handle the details of this excitation.

The first essential is some nuclear model for this  $2^+$  state. It was remarked in Sec. V that the level is almost certainly collective. Since this is not easily built into the present microscopic theory, we shall treat it rather as a particle-hole state, viz.,  $(p_{3/2})^{-1}(p_{1/2})$ . However, we should not be surprised if the theory then gives a

$^{27}$  S. I. Drozdov, Zh. Eksperim. i Teor. Fiz. **28**, 736 (1955) [English transl.: Soviet Phys.—JETP **1**, 588 (1955)].

poor description of the data. It should prove at least a useful pedagogic exercise.

The structure of the equations is very similar to that for elastic scattering. For example, if a proton undergoes the transition, then, in analogy with Eq. (5.20),

$$\langle \Gamma_N \rangle = - \| O_n \| x \| O_p' \|. \quad (6.1)$$

The one is missing because the excited state is orthogonal to the ground state. The  $O_n$  is the same  $6 \times 6$  matrix that we come across for the elastic case. However, since one of the protons is removed from the  $p_{3/2}$  and put into a  $p_{1/2}$  orbit,  $O_p'$  is a similar  $6 \times 6$  matrix but with one of its  $p_{3/2}$  columns replaced by a  $p_{1/2}$  one. It just resolves to choosing the appropriate  $6 \times 6$  minor of the  $8 \times 8$  matrix of Eq. (C6).

Since the excited state has  $T=0$ , its isospin structure is  $\frac{1}{2}\sqrt{2}(p\bar{p}+n\bar{n})$ . In the absence of charge-exchange effects, the amplitude for exciting the proton particle hole is the same as that for the neutron. We can, therefore, just consider the proton excitation, provided that we multiply the resulting cross section by 2. The considerable complications that arise in describing this process are due to the spin of the excited nucleus. Because of this, there are five possible orientations of the final state which we shall denote by

$$\begin{aligned} M=2: & \quad |p_{\frac{3}{2}}^{-\frac{3}{2}}\rangle^{-1} |p_{\frac{1}{2}}^{\frac{1}{2}}\rangle, \\ M=1: & \quad \frac{1}{2} |p_{\frac{3}{2}}^{-\frac{3}{2}}\rangle^{-1} |p_{\frac{1}{2}}^{-\frac{1}{2}}\rangle \\ & \quad + \frac{1}{2}\sqrt{3} |p_{\frac{3}{2}}^{-\frac{1}{2}}\rangle^{-1} |p_{\frac{1}{2}}^{\frac{1}{2}}\rangle, \\ M=0: & \quad \frac{1}{2}\sqrt{2} |p_{\frac{3}{2}}^{-\frac{1}{2}}\rangle^{-1} |p_{\frac{1}{2}}^{-\frac{1}{2}}\rangle \\ & \quad + \frac{1}{2}\sqrt{2} |p_{\frac{3}{2}}^{\frac{1}{2}}\rangle^{-1} |p_{\frac{1}{2}}^{\frac{1}{2}}\rangle, \\ M=-1: & \quad \frac{1}{2} |p_{\frac{3}{2}}^{-\frac{3}{2}}\rangle^{-1} |p_{\frac{1}{2}}^{\frac{1}{2}}\rangle \\ & \quad + \frac{1}{2}\sqrt{3} |p_{\frac{3}{2}}^{\frac{1}{2}}\rangle^{-1} |p_{\frac{1}{2}}^{-\frac{1}{2}}\rangle, \\ M=-2: & \quad |p_{\frac{3}{2}}^{\frac{3}{2}}\rangle^{-1} |p_{\frac{1}{2}}^{-\frac{1}{2}}\rangle. \end{aligned} \quad (6.2)$$

These are to be interpreted under the following convention: The amplitude, associated, for example, with the  $\Delta M=2$  transition, is to be obtained by taking the determinant of the  $6 \times 6$  minor derived from  $O$  [cf. Eq. (C6)] by eliminating the two  $\langle p_{\frac{1}{2}} |$  rows and also the  $|p_{\frac{3}{2}}^{-\frac{3}{2}}\rangle$  and  $|p_{\frac{1}{2}}^{-\frac{1}{2}}\rangle$  columns.

In this way we shall derive five different amplitudes, and since experimentally the polarization is not observed, the final cross section is the sum over all the spin orientations:

$$\frac{d\sigma}{d\Omega} = \sum_M |F_M|^2. \quad (6.3)$$

Although the differential cross section is axially symmetric, in contrast to the elastic case  $F_M$  will depend, in general, also on the direction of  $\mathbf{q}$ . This implies that  $\langle \Gamma_N \rangle_M$  will depend upon the direction of  $\mathbf{b}$  as well as its magnitude, which makes the calculation much more tedious. We have to consider  $\mathbf{b}$  as making some arbitrary

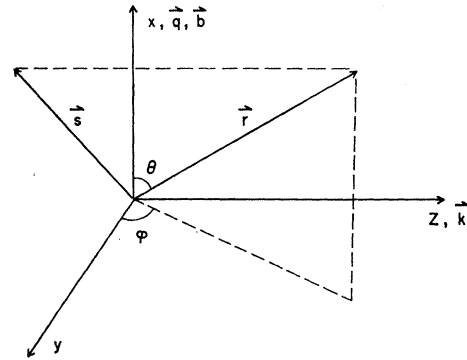


FIG. 16. Coordinate system used to evaluate the  $C^{12}(p,p')C^{12*}$  reaction.

angle  $\chi$  with the  $x$  axis (see Fig. 16), so that

$$\begin{aligned} b_x &= b \cos \chi, \\ b_y &= b \sin \chi, \end{aligned} \quad (6.4)$$

and the scattering operator becomes

$$\begin{aligned} \Gamma(b-s) &= (\sigma/4\pi\beta^2) \\ &\times \exp\{-([\mathbf{b} \cos \chi - x]^2 + [b \sin \chi - y]^2)/2\beta^2\}. \end{aligned} \quad (6.5)$$

The presence in this operator of terms odd in  $\cos \varphi$  induces transitions also of the form  $\Delta M = \text{odd}$ . For this reason the matrix  $O$  does not factorize and we must consider the more complicated (C6), where the  $\omega_i$  ( $i=1, \dots, 7$ ) are given by (C4). It is from this matrix that the appropriate minors must be procured.

There is one additional complication. Because  $\langle \Gamma_N \rangle_M$  is not axially symmetric, one cannot reduce the impact-parameter transform to a single Bessel transform. It must be left in the form

$$F_M(\mathbf{q}) = \frac{ik}{2\pi} \int_0^\infty b db \int_{-\pi}^{+\pi} d\chi e^{iqb \cos \chi} \langle \Gamma_N \rangle_M. \quad (6.6)$$

Note that in Eq. (6.6) we have let  $q$  lie along the  $x$  axis, because the unpolarized cross section is obviously independent of the direction.

In performing the  $\chi$  integration it is important to realize that  $\langle \Gamma_N \rangle_M$  is a polynomial in  $\sin \chi$  and  $\cos \chi$ . We can go much further than this though. Under the transformation  $\chi \rightarrow -\chi$ , we have from Eq. (3.4)

$$\begin{aligned} \omega_{1,2,3,4,5} &\rightarrow +\omega_{1,2,3,4,5}, \\ \omega_{6,7} &\rightarrow -\omega_{6,7}. \end{aligned} \quad (6.7)$$

The array  $\tilde{O}$  obtained from  $O$  by this transformation may be brought back to the original state by multiplying the following rows and columns by  $-1$ :

$$R_1, R_2, R_3, R_4; \quad C_1, C_2, C_3, C_4. \quad (6.8)$$

The total  $8 \times 8$  determinant is invariant under this transformation and is, therefore, an even function of  $\chi$  (it is, of course, independent of  $\chi$ ). However, some of

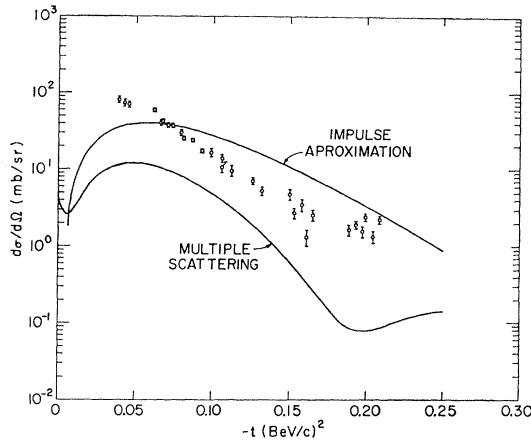


FIG. 17. Cross section for the excitation of the first  $2^+$  level (4.4 MeV) in  $C^{12}$  with 1-BeV protons; the experimental data are from Ref. 2. The impulse-approximation and multiple-scattering curves are calculated with the following parameters:  $\sigma = 44$  mb,  $\rho = -0.275$ ,  $\beta^2 = 5.45$  (BeV/c) $^2$ , and  $\alpha^2 = 0.401$  F $^{-2}$ .

the subdeterminants do change, from which we can deduce whether they are even or odd in  $\chi$ .

Secondly, under the transformation  $\chi \rightarrow \chi + \pi$ ,

$$\begin{aligned} \omega_{1,2,3,5,7} &\rightarrow \omega_{1,2,3,5,7}, \\ \omega_{4,6} &\rightarrow -\omega_{4,6}. \end{aligned} \quad (6.9)$$

This provides more restrictions on the subdeterminants and we eventually find

$$\begin{aligned} \langle \Gamma_N \rangle_{M=\text{even}} &= H_M(\cos^2\chi), \\ \langle \Gamma_N \rangle_{M=\text{odd}} &= \sin\chi \cos\chi H_M(\cos^2\chi), \end{aligned} \quad (6.10)$$

where  $H_M(a)$  is a polynomial in  $a$ .

Now it is easily seen from (6.6) that functions which are odd in  $\sin\chi$  integrate to zero. With this choice of the  $\mathbf{q}$  axis, then, we find that the odd  $M$  states are not excited. Furthermore, from looking at the powers of  $\cos\chi$  which occur in the determinant, it seems that we can end up with fifth-order polynomials in  $\cos^2\chi$ . In fact, there are very strong cancelations such that there is at most a linear term in  $\cos^2\chi$ . This follows from angular momentum conservation. If instead of calculating the amplitudes for excitation with a definite  $M$ , we had used helicity states  $\lambda$ , then since no orientation in space is fixed, the amplitudes could have at most a trivial dependence on  $\chi$ . Now the  $M$  amplitudes can be derived from the equivalent  $\lambda$  amplitudes by making a rotation through an angle  $\chi$ , which introduces factors of  $d_{\lambda M}^2(\chi)$  which have at most a  $\cos^2\chi$  term in them. Hence

$$\langle \Gamma_N \rangle_{M=\text{even}} = a_1^M + a_2^M \cos 2\chi, \quad (6.11)$$

where  $a_1$  and  $a_2$  are independent of  $\chi$ . Substituting this representation into (6.6), we get

$$F_M(\mathbf{q}) = ik \int_0^\infty b db [a_1^M J_0(qb) - a_2^M J_2(qb)]. \quad (6.12)$$

Since by symmetry  $F_2(q) = F_{-2}(q)$ , we have only two transition amplitudes to evaluate.

Two interesting results follow if we calculate the  $F_M$  in impulse approximation. Firstly,

$$F_2(q) = 0 \quad (6.13)$$

follows because we have taken  $\mathbf{q}$  to lie along the quantization axis. Even allowing for spin flip, the maximum change in angular momentum in this direction for a single nucleon is  $\Delta M = 1$ , which can not engender the excitation of the nuclear level with  $\Delta M = 2$ . Secondly, conservation of angular momentum in the  $z$  direction for forward scattering leads to the following relation between the two amplitudes:

$$F_2(0) = -(\sqrt{\frac{2}{3}})F_0(0). \quad (6.14)$$

In impulse approximation (6.13) then implies

$$F_0(0) = 0. \quad (6.15)$$

Equation (6.15) follows also from the orthogonality of initial and final states. Consequently, the greatest change between the predictions of the single- and multiple-scattering theories is in the forward direction, since the latter are not subject to the conditions (6.13) and (6.15).

The amplitudes were calculated by a numerical integration of Eq. (6.12) and the unpolarized cross section is shown in Fig. 17 together with the predictions of the impulse approximation. The comparison of theory with experiment is rather discouraging, being a factor of 4 too low. It is unlikely that the introduction of a spin dependence in the nucleon amplitude would affect the result radically since the  $2^+$  state can only be reached in second order. At lower energies, distorted-wave impulse approximation (DWIA) calculations<sup>28</sup> for proton excitation of this level are also too small by at least a factor of 3 if the same simple particle-hole model is used. A similar situation arises in electron excitation of the state.<sup>29</sup> Considerable improvement is obtained if configuration mixing is introduced, and this is almost certainly the case here. Work is, at present, in progress on the introduction of a more realistic wave function for  $C^{12}$ , with the aim of understanding better the elastic scattering and the  $2^+$  production reaction.

## VII. ELASTIC SCATTERING FROM DEUTERIUM

Since the whole of Glauber's theory was first derived to explain cross sections in deuterium, it may seem strange to have left this case to the last. It has, however, been often discussed in the literature and so will be treated in correspondingly less detail. Furthermore, we shall here come across additional complications, which are not so important elsewhere.

<sup>28</sup> R. Haybron and H. McManus, Phys. Rev. **140**, B638 (1965).  
<sup>29</sup> M. Bouten and P. Van Leuven, Ann. Phys. (N. Y.) **43**, 421 (1967).

We go back to the basic formula (2.13) and use the conventional definition of the deuteron wave function

$$\varphi(\mathbf{r}) = \psi(\mathbf{r}_1, \mathbf{r}_2), \quad (7.1)$$

where  $\mathbf{r} = (\mathbf{r}_1 - \mathbf{r}_2)$  is the internucleon separation. We shall neglect the small  $d$ -state probability so that  $\varphi(\mathbf{r})$  is then spherically symmetric. After changing the integration variable to  $\mathbf{r}$ , expanding the product in multiple scatterings and performing the integral over  $b$ , we obtain

$$F_{fi}(\mathbf{q}) = \int d^3r \varphi_f^*(\mathbf{r}) \varphi_i(\mathbf{r}) \times \left[ \exp\left(\frac{1}{2}i\mathbf{q} \cdot \mathbf{s}\right) f_n(\mathbf{q}) + \exp\left(-\frac{1}{2}i\mathbf{q} \cdot \mathbf{s}\right) f_p(\mathbf{q}) + \frac{i}{2\pi k} \int \exp(i\mathbf{q}' \cdot \mathbf{s}) f_n(\mathbf{q} + \frac{1}{2}\mathbf{q}) f_p(\mathbf{q}' - \frac{1}{2}\mathbf{q}) \right]. \quad (7.2)$$

The factors of  $\frac{1}{2}$  occurring in the exponents arise because  $r$  is equated to the diameter of the deuteron rather than the radius. For elastic scattering, define the deuteron form factor

$$S(\mathbf{q}) = \int d^3r e^{i\mathbf{q} \cdot \mathbf{s}} |\varphi(\mathbf{r})|^2. \quad (7.3)$$

In terms of this function, the elastic amplitude (7.2) becomes

$$F_{ii}(\mathbf{q}) = f_n(\mathbf{q})S(\frac{1}{2}\mathbf{q}) + f_p(\mathbf{q})S(-\frac{1}{2}\mathbf{q}) + \frac{i}{2\pi k} \int S(\mathbf{q}') f_n(\frac{1}{2}\mathbf{q} + \mathbf{q}') f_p(\frac{1}{2}\mathbf{q} - \mathbf{q}') d^{(2)}\mathbf{q}'. \quad (7.4)$$

As was demonstrated in Sec. III, charge-exchange effects can be included by replacing  $f_n f_p$  by  $f_n f_p - \frac{1}{2}(f_n - f_p)^2$  to obtain

$$F(\mathbf{q}) = f_n(\mathbf{q})S(\frac{1}{2}\mathbf{q}) + f_p(\mathbf{q})S(-\frac{1}{2}\mathbf{q}) + \frac{i}{2\pi k} \int S(\mathbf{q}') d^{(2)}\mathbf{q}' \{ f_n(\frac{1}{2}\mathbf{q} + \mathbf{q}') f_p(\frac{1}{2}\mathbf{q} - \mathbf{q}') - \frac{1}{2}[(f_p(\frac{1}{2}\mathbf{q} + \mathbf{q}') - f_n(\frac{1}{2}\mathbf{q} + \mathbf{q}')) \times (f_n(\frac{1}{2}\mathbf{q} - \mathbf{q}') - f_p(\frac{1}{2}\mathbf{q} - \mathbf{q}'))] \}. \quad (7.5)$$

From analyses of low-energy nucleon-nucleon data, numerical deuteron wave functions have been derived. Since these are only tabulated for discrete values of  $r$ , an interpolation is required in order to perform the integrals in (7.3) and (7.5). Using as a basis the expansion

$$\varphi(\mathbf{r}) = - \sum_r C_i e^{-\mu_i r}, \quad (7.6)$$

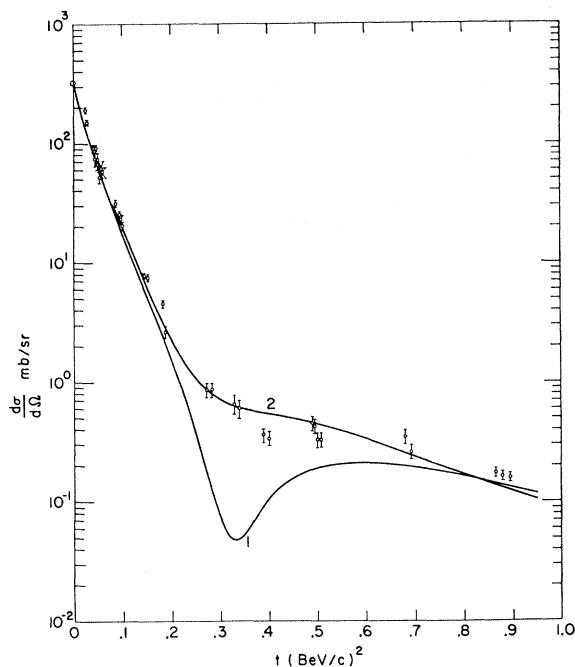


FIG. 18. Elastic proton-deuteron cross section at 1 BeV; the experimental data are from Ref. 2. The theoretical curves result from a multiple-scattering calculation, with  $\sigma_P = 47.5$  mb,  $\sigma_n = 40.4$  mb,  $\rho_P = -0.05$ ,  $\rho_n = -0.5$ ,  $\beta^2 = 5.45$  (BeV/c) $^{-2}$ , and the deuteron wave function of Ref. 31. A sharp minimum is then predicted at  $t \sim -0.35$  (BeV/c) $^2$ , but this can be washed away by letting the relative real parts of the nuclear amplitudes vary with angle. The value  $\xi = 0.3 F^2$  is from Eq. (7.10).

Moravcsik<sup>30</sup> and McGee<sup>31</sup> were able to reproduce well the tabulated  $s$ -wave functions of Gartenhaus<sup>32</sup> and of Hamada and Johnston,<sup>33</sup> respectively. With this interpolatory function, the integral for the form factor (7.3) can be evaluated analytically. One has then only a two-dimensional integral of (7.5) to perform numerically.

The high-energy nucleon-nucleon amplitudes are represented as in the previous sections [see (4.3) and (4.4)], and the result of using them in (7.5) is shown in Fig. 18 together with the Brookhaven experimental data.<sup>2</sup> The agreement between the two is reasonable in the vicinity of the primary and secondary maxima, but for  $q^2 \sim 0.35$  (BeV/c) $^2$  the theory predicts a sharp minimum, whereas only a change in slope is found experimentally. This marked discord persists if (a) the interpolation of Moravcsik or McGee is used (in fact, they give extremely close answers), (b) a quadratic term is introduced in the exponent describing the nucleon-nucleon amplitudes, as in Eq. (4.2), and (c)  $\sigma_n$  and  $\sigma_p$  are varied while keeping the total  $p$ - $d$  cross section roughly constant around the value obtained by Bugg *et al.*<sup>17</sup> In the absence of spin dependence, the

<sup>30</sup> M. J. Moravcsik, Nucl. Phys. 7, 113 (1958).

<sup>31</sup> I. McGee, Phys. Rev. 151, 772 (1966).

<sup>32</sup> S. Gartenhaus, Phys. Rev. 100, 900 (1956).

<sup>33</sup> T. Hamada and I. D. Johnston, Nucl. Phys. 34, 382 (1962).

small  $d$ -state admixture in the deuteron wave function can have but little influence.

It has been previously stressed that the depth of the minimum is a very sensitive function of the relative real parts of the nucleon amplitudes, and so one is led to the question of the angular constancy of  $\rho$ . For instance, if we take  $\rho_p = \rho_n = -0.9$  then the predicted minimum is washed out and reasonable agreement with the data obtained in this region. Let us therefore try a quadratic dependence of  $\rho$  upon  $q^2$ :

$$\rho_p(q^2) = \sum_{m=0}^2 \rho_p^{(m)} q^{2m}, \quad (7.7)$$

and similarly for the neutron. The zeroth-order coefficients are obtained from the dispersion relation values of  $\rho$ . The other coefficients were varied subject to the constraints that the average  $\rho$  be about  $-0.3$  or  $0.4$  for  $q^2 \sim 0.23$  (BeV/c)<sup>2</sup> (the He<sup>4</sup> minimum) and  $-0.9$  for  $q^2 \sim 0.35$  (BeV/c)<sup>2</sup> (the deuterium minimum). In this way we arrive at the somewhat surprising result that the theoretical minimum is actually deepened. This can be understood in the following way. In general, both the real and imaginary parts of the total amplitude (7.5) each have a zero, although up to now we have thought mainly about the latter. In the constant  $\rho$  approximation (say,  $\rho \sim -0.9$ ), these zeros are far apart. If  $\rho$  is allowed to vary with angle the single-scattering amplitude depends on the value of  $\rho$  for a particular value  $q$ , whereas the double is sensitive to a whole range of momentum transfers clustered about  $\frac{1}{2}q$ . This allows the zeros to move relative to each other as functions of the coefficients in expansion (7.7) and the above conditions allow them to come quite close together. Consequently, the average real part of the deuteron amplitude can be rather large on the average (larger, say, than that predicted using the dispersion-relation values of  $\rho$ ), but in the vicinity of the minimum it is accidentally small.

It may well be that  $\rho$  varies much faster than was allowed for by the previous considerations, in which case it is important to ensure that the chosen parametrization still reproduces the proton-proton cross section. This is most easily achieved by taking<sup>34</sup>

$$f_{pp}(q) = (ik\sigma/4\pi)(1 - i\rho)e^{-\beta^2 q^2/2} e^{i h(q)}, \quad (7.8)$$

where  $h(q)$  is a real function with

$$h(0) = 0. \quad (7.9)$$

The simplest such function is

$$h(q) = \zeta q^2, \quad (7.10)$$

and we shall try this for both the proton and the neutron with the same value of  $\zeta$ . This value was varied and it was found that a reasonable description of the deuterium data required at least  $\zeta = 0.25$  or  $3.3$  F<sup>2</sup>

(see Fig. 18). This is so large that the amplitude for  $t = -0.35$  (BeV/c)<sup>2</sup> is almost completely out of phase with that for  $t = 0$ . We cannot rule out such a rapid phase variation *a priori*, but its existence must disfigure the essential simplicity of the discussion in the present paper. Happily we can state that with  $\zeta \sim 0.3$  F<sup>2</sup> the minimum in He<sup>4</sup> completely disappears, so that we are forced to seek an alternative explanation of the deuterium experiment.

The most important qualitative difference between O<sup>16</sup>, C<sup>12</sup>, and He<sup>4</sup>, on the one hand, and H<sup>2</sup> on the other is that while the former have spin 0, the latter has spin 1. Now there is quite strong experimental evidence that there is a spin dependence in the proton-proton amplitude even at this high energy. Recent small-angle proton-proton data at this energy,<sup>16</sup> extrapolated to the forward direction after the removal of the Coulomb contribution, lie 25% above the optical point. A spin dependence of the nucleon-nucleon amplitude is much more important for deuterium than for the other nuclei. To see this, consider the following oversimple model. If we neglect the spin of the fast proton, the cross section in helium is just the absolute square of a quantity which can have strong cancellations at a particular angle. However, the deuterium cross section is the incoherent sum of three partial cross sections corresponding to no spin flip, spin flip of one unit, and spin flip of two. Unless *either* each of these partial cross sections has a minimum at about the same angle, *or* one of the cross sections completely dominates the other two, then no very sharp minimum would be expected. If this is, indeed, the explanation of the shallowness observed, a sharp minimum could be detected only in an experiment with a polarized target where the final polarization is also measured. This effectively rules out the use of the deuteron to measure  $\rho$ , as has been recently suggested.<sup>35</sup> It is necessary to test this line of reasoning by introducing an explicit model of the nucleon-nucleon spin dependence which fits the available data. One must then show that the minimum is not destroyed in He<sup>4</sup>, whereas it is in deuterium. Care must be taken with this latter because if we assume

$$f_{pp} = a + b\sigma \cdot (\mathbf{q} \times \mathbf{k}), \quad (7.11)$$

then a strong cancellation takes place if we let  $a$  and  $b$  have the same angular form  $\exp(-\frac{1}{2}b^2 q^2)$ .

All that can be said at the present is that if there is a background of 25% of the impulse approximation due to spin dependence (see Sec. IV), then this would fill up the minimum considerably.

The situation should be clarified when experiments are performed on high-energy elastic pion-deuteron scattering. There are many advantages in doing this experiment rather than the analogous proton experiment. From charge symmetry we have direct informa-

<sup>34</sup> V. Franco and R. J. Glauber (private communication).

<sup>35</sup> L. Bertocchi, Nuovo Cimento **50A**, 1015 (1967); J. Formanek and J. S. Trefil, Nucl. Phys. **B3**, 155 (1967).

tion on the pion-neutron interaction. Furthermore, because of its simpler spin structure, reliable phase-shift analyses have been pushed to a much higher energy than for proton-proton. Thus, if experiments are performed at about 1 GeV we should have all the information necessary to analyze them.

### VIII. CONCLUSIONS

It is apparent from the results of the previous sections that high-energy protons are a very useful complement to electrons in the investigation of nuclear structure. This follows because experimental techniques have reached such a high precision and because in the Glauber model we have a theoretical tool which seems capable of handling at least the small-angle elastic scatterings. There are many doubtful assumptions in this theory which warrant further investigation, but the ultimate test of the approach must lie in continued comparison with experiment. In the cases looked at in this work, such a comparison has been very encouraging. In the main the discrepancies with the data have, we hope, been understood. The most remarkable agreement has been obtained for  $O^{16}$ , where we believed *a priori* that we had a reasonable nuclear model. The deviations in  $C^{12}$  could then be laid at the feet of the nuclear physics, rather than the scattering theory, and so the present work can be considered as some confirmation of the strong deformation in this nucleus. The results on the excitation of the low-lying  $2^+$  state in  $C^{12}$  have much in common with the electron and lower-energy proton data. The theoretical curve has the same general shape as that observed, but is too low by a factor of about 4. It is very important to try to improve upon this by taking better nuclear wave functions which have proved themselves elsewhere. There were many other nuclear transitions measured, but not clearly separated, in the Brookhaven experiment, and these too remain to be investigated.

It was found that in  $He^4$  correlations do not seem to play an important role and a good fit to both the electron and proton observations could be obtained by modifying the single-particle density. The attempt to explain the results by keeping the Gaussian single-particle density and introducing a Jastrow correlation function was a failure. This may, however, be due to the rather soft nature of the damping used. A form which should then be tried is  $(1 - e^{-\delta^2 r_{ij}^2})^n$ , since for large  $n$  this kills the wave function very strongly at small separations, but still leads to integrals which can be performed analytically. It is mainly a question of extending the bookkeeping.

The deuterium analysis seems at first disappointing, but if, as we have speculated, this is due to spin dependence, then, from the study of proton-deuteron scattering, we may learn something about the spin structure of the proton-proton amplitude. A similar difficulty may be present in simplified quark models for

nucleon-nucleon scattering.<sup>36</sup> The situation should be clearer after the measurement of pion-nucleus scattering and the subsequent analysis. Other useful proton experiments would include the scattering from  $He^3$  and  $Li^6$ , both having spin and both in their own way interesting nuclei.

Even away from the diffraction minimum, the neglect of spin dependence is much more important for deuterium than for the other nuclei. Since  $He^4$  has spin 0, target-nucleon spin flips cannot occur singly. Consequently, spin flip should not be important until the secondary maximum. Even there they are suppressed somewhat with respect to the non-spin-flip term by combinatorial factors. For deuterium, spin flip can occur even in the impulse approximation.

Note that we have not looked at, for example, the  $(p,2p)$  reactions. This should provide much more information about correlations in the nucleus, but additional work must be done on the theory before it is capable of treating such problems. The same remark applied to the  $(p,d)$  process, where a high-energy deuteron is seen to emerge. It is likely that the deuteron-production reactions will not really be understood until we have a good model for high-energy backward elastic proton-deuteron scattering. This is still lacking.

### ACKNOWLEDGMENTS

We wish to acknowledge the valuable help from, and discussions with, H. Palevsky, J. L. Friedes, G. W. Bennet, N. S. Wall, R. F. Peierls, A. H. Mueller, B. R. Martin, R. J. Glauber, V. Franco, V. J. Emery, S. Kahana, P. Gugelot, and T. Cogley.

### APPENDIX A

We here illustrate the method of calculating charge-exchange effects for proton scattering from  $He^4$ , analogous to the deuteron case described by Eq. (3.4). Denote the target nucleons by  $p_1(n_1)$  for the proton (neutron) with spin up and  $p_2(n_2)$  with spin down. Since by assumption the nucleon-nucleon amplitude is spin-independent, the only charge exchanges which need be considered are those between  $p_1$  and  $n_1$  and between  $p_2$  and  $n_2$ .

There are 12 elastic double-scattering terms of which six are  $p_1p_2$ ,  $p_1n_2$ ,  $p_1n_1$ ,  $n_1p_1$ ,  $n_1p_2$ , and  $n_1n_2$ . The other six are obtained by interchanging the labels 1 and 2. A double charge exchange can only arise if the first nucleon is a neutron and the subscripts are the same, viz., for the combinations  $n_1p_1$  and  $n_2p_2$ . Now a neutron-proton system with spins aligned must be in a state with  $T=0$ . Hence, as was argued in Sec. III, the amplitude must be odd under the interchange  $n_i \leftrightarrow p_i$ .

<sup>36</sup> D. Harrington and A. Pagnamenta, Phys. Rev. Letters 18, 1147 (1967).

The double-scattering terms should be modified to be

$$F_2 \sim 2f_p^2 + 2f_n^2 + 8f_p f_n \rightarrow 2f_p^2 + 2f_n^2 + 8f_p f_n - 2(f^{c.e.})^2. \quad (\text{A1})$$

But

$$f^{c.e.} = f_p - f_n, \quad (\text{A2})$$

so that

$$F_2 \sim 12f_p f_n. \quad (\text{A3})$$

Similar counting techniques lead easily to the correct expressions for triple and quadruple scattering. They are

$$F_3 \sim 12(f_p + f_n)f_p f_n - 6(f_p^2 + f_n^2)(f^{c.e.})^2, \quad (\text{A4})$$

$$F_4 \sim 24f_p^2 f_n^2 - 4(f_p^2 + f_n^2 + 4f_p f_n)(f^{c.e.})^2 + 2(f^{c.e.})^4. \quad (\text{A5})$$

### APPENDIX B

In the evaluation of the scattering amplitude for  $\text{He}^4$  in Sec. IV, considerable attention was paid to integrals of the form

$$I = \int d^3r_1 d^3r_2 d^3r_3 \exp[-(\mathbf{r}_1, \mathbf{r}_2, \mathbf{r}_3)A^{(3)}(\mathbf{r}_1, \mathbf{r}_2, \mathbf{r}_3)^T] \times \exp[-(\mathbf{s}_1, \mathbf{s}_2, \mathbf{s}_3, i\mathbf{q})B^{(4)}(\mathbf{s}_1, \mathbf{s}_2, \mathbf{s}_3, i\mathbf{q})^T], \quad (\text{B1})$$

where  $A^{(3)}$  is a  $3 \times 3$  and  $B^{(4)}$  is a  $4 \times 4$  real symmetric matrix. Also the  $\mathbf{s}_i$  are the components of the  $\mathbf{r}_i$  in the  $x$ - $y$  plane. Let us then first calculate the  $z_i$  integrals which depend only on the  $A^{(3)}$  matrix.

$$I_z = \int dz_1 dz_2 dz_3 \exp[-(z_1, z_2, z_3)A^{(3)}(z_1, z_2, z_3)^T]. \quad (\text{B2})$$

The transformation into another basis wherein  $A^{(3)}$  is diagonal can be effected by a unitary matrix, so that the corresponding Jacobian is unity. Then (B2) becomes

$$I_z = \int dz_1' dz_2' dz_3' \exp(-\lambda_i z_i'^2) = \frac{\pi^{3/2}}{(\lambda_1 \lambda_2 \lambda_3)^{1/2}}, \quad (\text{B3})$$

where the  $\lambda_i$  are the eigenvalues of  $A^{(3)}$ . Since only their product occurs in (B3), the result can be simplified:

$$I_z = \pi^{3/2} / \|A^{(3)}\|^{1/2}. \quad (\text{B4})$$

There remain the  $x$ - $y$  integrations

$$I_{xy} = \int d^3\mathbf{s}_1 d^3\mathbf{s}_2 d^2\mathbf{s}_3 \times \exp[-(\mathbf{s}_1, \mathbf{s}_2, \mathbf{s}_3, i\mathbf{q})C^{(4)}(\mathbf{s}_1, \mathbf{s}_2, \mathbf{s}_3, i\mathbf{q})^T]. \quad (\text{B5})$$

Here  $C^{(4)}$  is a symmetric real  $4 \times 4$  matrix defined by

$$C_{ij}^{(4)} = A_{ij}^{(3)} + B_{ij}^{(4)}, \quad i, j = 1, 2, 3 \\ = B_{ij}^{(4)} \quad \text{otherwise.} \quad (\text{B6})$$

We go over to a new basis via the transformation

$$\mathbf{s}_i = \mathbf{t}_i + i\beta_i \mathbf{q} \quad (\text{B7})$$

such that the cross terms between  $\mathbf{q}$  and the coordinates disappear. The quadratic form becomes

$$= C_{ij}^{(4)} \mathbf{s}_i \cdot \mathbf{s}_j + 2iC_{i4}^{(4)} \mathbf{s}_i \cdot \mathbf{q} - C_{44}^{(4)} q^2 \\ = C_{ij}^{(4)} \mathbf{t}_i \cdot \mathbf{t}_j + i\mathbf{t}_i \cdot \mathbf{q} (2C_{i4}^{(4)} + 2\beta_j C_{ij}^{(4)}) \\ - (C_{44}^{(4)} + 2\beta_i C_{i4}^{(4)} + C_{ij}^{(4)} \beta_i \beta_j) q^2, \quad (\text{B8})$$

where the summation is over  $i, j = 1, 2, 3$ .

In order that the cross terms vanish,

$$B_j C_{ij}^{(4)} = -C_{i4}^{(4)}. \quad (\text{B9})$$

If  $C^{(3)}$  is the north-west submatrix of  $C^{(4)}$ , then

$$B_j = -(C^{(3)-1})_{ji} C_{i4}^{(4)}. \quad (\text{B10})$$

Using this condition, the coefficient of the  $q^2$  term becomes

$$- [C_{44}^{(4)} - (C^{(3)-1})_{ji} C_{i4}^{(4)} C_{j4}^{(4)}] \\ = - [C_{44}^{(4)} \|C^{(3)}\| \\ - (\text{Adj} C^{(3)})_{ij} C_{i4}^{(4)} C_{j4}^{(4)}] / \|C^{(3)}\| \\ = - \|C^{(4)}\| / \|C^{(3)}\|. \quad (\text{B11})$$

All that remains is the normalization integral, which can be done as for the  $z$  case. Thus

$$I = \frac{\pi^{9/2}}{\|A^{(3)}\|^{1/2} \|A^{(3)} + B^{(3)}\|} \exp\left(\frac{\|A^{(4)} + B^{(4)}\|}{\|A^{(3)} + B^{(3)}\|} q^2\right). \quad (\text{B12})$$

### APPENDIX C

The inclusion of the Pauli principle in Sec. V for elastic scattering from  $\text{C}^{12}$  and  $\text{O}^{16}$ , and in Sec. VI for the excitation of the  $\text{C}^{12}$  nucleus, necessitates the introduction of an  $8 \times 8$  matrix  $O$ . We discuss first the general case of Sec. VI, where the impact parameter  $\mathbf{b}$  makes an angle  $\chi$  with the  $x$  axis. In this frame the scattering operator is

$$\Gamma(\mathbf{b} - s_j) = (\sigma_j / 4\pi\beta^2) \\ \times \exp[-(b \cos\chi - x_j)^2 + (b \sin\chi - y_j)^2 / 2\beta^2]. \quad (\text{C1})$$

Let us define the various projections of this operator by

$$A(L, M; L', M') = N_L N_{L'} \int d^3r \Gamma(\mathbf{b} - \mathbf{s}) r^{L+L'} \\ \times e^{-\alpha^2 r^2} Y_{L, M}^* Y_{L', M'}, \quad (\text{C2})$$

where

$$N_0 = (4\alpha^3 / \pi^{1/2})^{1/2}, \quad N_1 = (8\alpha^5 / 3\pi^{1/2})^{1/2}. \quad (\text{C3})$$

The elements of  $O$  are just linear combinations of the

$A$ 's. Explicitly,

$$\begin{aligned}\omega_1 &= A(0,0;0,0) = \frac{\sigma}{2\pi} \frac{\alpha^2}{(1+2\alpha^2\beta^2)} E, \\ \omega_2 &= A(1,1;1,1) = \frac{\sigma\alpha^2}{4\pi} \left[ \frac{1}{(1+2\alpha^2\beta^2)} + \frac{2\alpha^2\beta^2}{(1+2\alpha^2\beta^2)^2} + \frac{2\alpha^2b^2 \sin^2\chi}{(1+2\alpha^2\beta^2)^3} \right] E, \\ \omega_3 &= A(1,0;1,0) = \frac{\sigma\alpha^4}{\pi} \left[ \frac{\beta^2}{(1+2\alpha^2\beta^2)^2} + \frac{b^2 \cos^2\chi}{(1+2\alpha^2\beta^2)^3} \right] E, \tag{C4}\end{aligned}$$

$$\begin{aligned}\omega_4 &= A(1,0;0,0) = \frac{\sigma}{\pi(2)^{1/2}} \frac{\alpha^3b \cos\chi}{(1+2\alpha^2\beta^2)^2} E, \\ \omega_5 &= A(1,1;1,-1) = -\frac{\sigma\alpha^2}{4\pi} \left[ \frac{1}{(1+2\alpha^2\beta^2)^2} - \frac{2\alpha^2b^2 \sin^2\chi}{(1+2\alpha^2\beta^2)^3} \right] E, \\ \omega_6 &= -\frac{\sigma\alpha^3b \sin\chi}{2\pi(1+2\alpha^2\beta^2)^2} E, \\ \omega_7 &= -\frac{\sigma\alpha^4b^2 \sin\chi \cos\chi}{\pi(2)^{1/2}(1+2\alpha^2\beta^2)^3} E, \tag{C5}\end{aligned}$$

where  $E$  is an abbreviation for

$$E = \exp[-\alpha^2b^2/(1+2\alpha^2\beta^2)]. \tag{C6}$$

Then  $O$  becomes

$$\begin{array}{cccccccc|c} \langle S \frac{1}{2} \frac{1}{2} | & \langle P \frac{3}{2} \frac{1}{2} | & \langle P \frac{3}{2} -\frac{3}{2} | & \langle P \frac{1}{2} \frac{1}{2} | & \langle S \frac{1}{2} -\frac{1}{2} | & \langle P \frac{3}{2} \frac{3}{2} | & \langle P \frac{3}{2} -\frac{1}{2} | & \langle P \frac{1}{2} -\frac{1}{2} | & \\ 1-\omega_1 & -(\sqrt{\frac{2}{3}})\omega_4 & 0 & (\frac{1}{3}\sqrt{3})\omega_4 & 0 & -\omega_6 & \frac{1}{3}\sqrt{3}\omega_6 & -(\sqrt{\frac{2}{3}})\omega_6 & | S \frac{1}{2} \frac{1}{2} \rangle \\ -(\sqrt{\frac{2}{3}})\omega_4 & 1-\frac{2}{3}\omega_3-\frac{1}{3}\omega_2 & -\frac{1}{3}\sqrt{3}\omega_5 & -\frac{1}{3}\sqrt{2}(\omega_2-\omega_3) & -\frac{1}{3}\sqrt{3}\omega_6 & -(\sqrt{\frac{2}{3}})\omega_7 & 0 & -\omega_7 & | P \frac{3}{2} \frac{1}{2} \rangle \\ 0 & -\frac{1}{3}\sqrt{3}\omega_5 & 1-\omega_2 & -(\sqrt{\frac{2}{3}})\omega_5 & \omega_6 & 0 & (\sqrt{\frac{2}{3}})\omega_7 & \frac{1}{3}\sqrt{3}\omega_7 & | P \frac{3}{2} -\frac{3}{2} \rangle \\ \frac{1}{3}\sqrt{3}\omega_4 & -\frac{1}{3}\sqrt{2}(\omega_2-\omega_3) & -(\sqrt{\frac{2}{3}})\omega_5 & 1-\frac{2}{3}\omega_2-\frac{1}{3}\omega_3 & -(\sqrt{\frac{2}{3}})\omega_6 & \frac{1}{3}\sqrt{3}\omega_7 & -\omega_7 & 0 & | P \frac{1}{2} \frac{1}{2} \rangle \\ 0 & -\frac{1}{3}\sqrt{3}\omega_6 & \omega_6 & -(\sqrt{\frac{2}{3}})\omega_6 & 1-\omega_1 & 0 & -(\sqrt{\frac{2}{3}})\omega_4 & -\frac{1}{3}\sqrt{3}\omega_4 & | S \frac{1}{2} -\frac{1}{2} \rangle \\ -\omega_6 & -(\sqrt{\frac{2}{3}})\omega_7 & 0 & \frac{1}{3}\sqrt{3}\omega_7 & 0 & 1-\omega_2 & -\frac{1}{3}\sqrt{3}\omega_5 & (\sqrt{\frac{2}{3}})\omega_5 & | P \frac{3}{2} \frac{3}{2} \rangle \\ \frac{1}{3}\sqrt{3}\omega_6 & 0 & (\sqrt{\frac{2}{3}})\omega_7 & -\omega_7 & -(\sqrt{\frac{2}{3}})\omega_4 & -\frac{1}{3}\sqrt{3}\omega_5 & 1-\frac{2}{3}\omega_3-\frac{1}{3}\omega_2 & \frac{1}{3}\sqrt{2}(\omega_2-\omega_3) & | P \frac{3}{2} -\frac{1}{2} \rangle \\ -(\sqrt{\frac{2}{3}})\omega_6 & -\omega_7 & \frac{1}{3}\sqrt{3}\omega_7 & 0 & -\frac{1}{3}\sqrt{3}\omega_4 & (\sqrt{\frac{2}{3}})\omega_5 & \frac{1}{3}\sqrt{2}(\omega_2-\omega_3) & 1-\frac{2}{3}\omega_2-\frac{1}{3}\omega_3 & | P \frac{1}{2} -\frac{1}{2} \rangle. \end{array} \tag{C7}$$

For the spherically symmetric cases dealt with in Sec. V it is legitimate to take  $\mathbf{b}$  along the  $x$  axis, i.e.,  $\chi=0$ . This introduces enormous simplifications. The  $\omega_i$  reduce to

$$\begin{aligned}\omega_1 &= \frac{\sigma}{2\pi} \frac{\alpha^2}{(1+2\alpha^2\beta^2)} E, & \omega_2 &= \frac{\sigma\alpha^2}{4\pi} \left[ \frac{1}{(1+2\alpha^2\beta^2)} + \frac{2\alpha^2\beta^2}{(1+2\alpha^2\beta^2)^2} \right] E, & \omega_3 &= \frac{\sigma\alpha^4}{\pi} \left[ \frac{\beta^2}{(1+2\alpha^2\beta^2)^2} + \frac{b^2}{(1+2\alpha^2\beta^2)^3} \right] E, \\ \omega_4 &= \frac{\sigma}{\pi(2)^{1/2}} \frac{\alpha^3b}{(1+2\alpha^2\beta^2)^2} E, & \omega_5 &= -\frac{\sigma\alpha^2}{4\pi} \left[ \frac{1}{(1+2\alpha^2\beta^2)^2} \right] E, & \omega_6 &= 0, & \omega_7 &= 0.\end{aligned} \tag{C8}$$

The vanishing of  $\omega_6$  and  $\omega_7$  means that the matrix  $O$  decouples into two distinct  $4 \times 4$  submatrices, as can trivially be seen from (C7).